hematopoietic progenitors and, moreover, enforced expression of HLF in cytokine-dependent cells failed to inhibit apoptosis.[18,19] We then identified a bZIP factor, E4 promoter binding protein (E4BP4)/nuclear factor regulated by IL-3 (NFIL3) (Figure 1), as a physiologic counterpart of E2A-HLF. E4BP4 has nearly identical DNA-binding specificity to CES-2 and its expression is tightly regulated by interleukin (IL-3) in IL-3–dependent cell lines such as FL5.12 and Baf-3. Moreover, enforced expression of E4BP4 delays apoptosis of IL-3–deprived cells.[23,24] These data suggested that subversion of the roles of antiapoptotic bZIP factors normally regulated by cytokines is 1 critical aspect of leukemogenesis induced by E2A-HLF.

Other bZIP factors may also play important roles in the regulation of hematopoietic cell survival. HLF is a member of the proline- and acidic amino acid–rich (PAR) bZIP family, which also includes thyrotroph embryonic factor (TEF)[25] and albumin promoter D-box–binding protein (DBP)[26] (Figure 1). TEF was originally cloned as a factor expressed in the developing anterior pituitary gland that could *trans*-activate the *TSHβ* promoter,[25] whereas DBP was cloned as a liver-enriched transcriptional activator that binds to the D element of the albumin promoter.[26] It has been well documented that the PAR proteins as well as E4BP4 are implicated in circadian control.[27-33] PAR proteins may also be involved in the regulation of cell death because all 3 PAR proteins exhibit nearly identical DNA-binding specificity to that of E4BP4 and CES-2.[25,26,28,29,34-37] Here we demonstrate that TEF promotes the survival of FL5.12 cells due to IL-3 starvation. Unexpectedly, we also found that TEF potently represses the expression of the β subunits of the IL-3 receptor, blocking proliferation and leading to arrest of the cell cycle in the G_0/G_1 phase, even in the presence of IL-3.

Materials and methods

Constructs of eukaryotic expression vectors

Expression plasmids containing the cDNAs of wild-type *TEF* (pMT-TEF), a mutated *TEF* (pMT-TEF basic mutant [BX]), and *E2AHLF* (pMT–E2A-HLF) were constructed with the pMT-CB6$^+$ eukaryotic expression vector (a gift from F. Rauscher III, Wistar Institute, Philadelphia, PA), which contains the inserted cDNA under the control of a sheep metallothionein promoter as well as the neomycin resistance gene driven by the simian virus 40 early promoter. The cDNA encoding a basic mutant of TEF (TEF/BX) that contained substitutions for 6 of the amino acid residues in the basic region critical for DNA binding (TRRKKNNVAAK mutated to TSPKSYNVPPK; single-letter code) was made by polymerase chain reaction (PCR) mutagenesis.

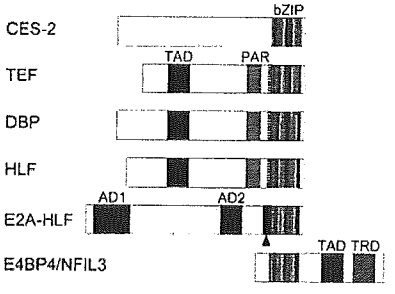

Figure 1. Schematic representation of the CES-2, TEF, DBP, HLF, E2A-HLF, and E4BP4/NFIL3 proteins. The CES-2 protein in *C elegans* contains a basic region/leucine zipper (bZIP) domain in the carboxyl-terminal region and acts as a transrepressor. TEF, DBP, and HLF contain a proline- and acidic amino acid–rich (PAR) domain as well as a bZIP domain in the carboxyl-terminal region, which shows high level of sequence identity to that of CES-2. TEF, DBP, and HLF each also contain a *trans*-activation domain (TAD) and can act as transcriptional activators. The E2A-HLF fusion protein, which is expressed in t(17;19)–positive leukemia cells, retains the 2 transactivation domains in the amino terminal of E2A (AD1 and AD2) but not its basic region/helix-loop-helix domain, which is replaced by the bZIP domain of HLF. E2A-HLF has a joining region (■ with arrowhead) generated at the breakpoint but not the basic region extension (BRE; indicated with ▤) nor the PAR domain of HLF, which contribute to sequence-specific DNA binding. E4BP4/NFIL3 contains a bZIP domain in its amino-terminal region and has nearly identical DNA-binding specificity as that of CES-2, TEF, DBP, HLF, and E2A-HLF. E4BP4 acts as either a transactivator or transrepressor depending on complexes formed by its TAD or transrepression domain (TRD) in its carboxyl-terminal region.

Cell culture and cell survival assay

FL5.12 cells, which are murine IL-3–dependent cells, were cultured in RPMI 1640 medium supplemented with 10% fetal calf serum and 0.5% 10T1/2 cell-conditioned medium as a source of IL-3. Transfectants were generated by electroporation using 2×10^7 cells and 80 μg of DNA with a gene pulser (Bio-Rad, Hercules, CA) set at 300 mV and 960 μF. Cells were then cultured in 24-well dishes and selected in the presence of the neomycin analog G418 (0.6 mg/mL) for 2 weeks. The induction of protein expression with Zn in G418-resistant cells was confirmed by immunoblot analysis. Cell growth and cell survival experiments were performed using 3 independent pools of cells, and the results of representative data of multiple experiments are shown. For cell survival assays, cells growing exponentially in IL-3–containing medium were precultured for 16 hours in the presence or absence of 100 μM $ZnSO_4$. Cells were washed with IL-3–free medium twice and were adjusted to 5×10^5 cells per milliliter. Viable cell counts were determined by trypan blue dye exclusion.

Immunoblot analysis

Cells were solubilized in Nonidet P-40 lysis buffer (150 mM NaCl, 1.0% Nonidet P-40, 50 mM Tris [tris(hydroxymethyl)aminomethane; pH 8.0]), and total cellular proteins were separated by sodium dodecyl sulfate–polyacrylamide gel electrophoresis. After wet electrotransfer onto polyvinylidene difluoride membranes, proteins were detected with the following primary antibodies: anti-HLF c-terminal (C),[35] anti-p44/42 mitogen-activated protein kinase (MAPK; New England BioLabs, Beverly, MA), anti-p70S6K (New England BioLabs), anti-Akt (New England BioLabs), antiphospho–signal transducers and activators of transcription 5 (anti–phospho-STAT5; Tyr694; New England BioLabs), anti–phospho-p44/42MAPK (Thr202/Tyr204; New England BioLabs), anti–phospho-p70S6K (Thr421/Ser424; New England BioLabs), and anti–phospho-Akt (Ser473; New England BioLabs) rabbit serum, or anti-β-tubulin (Pharmingen, San Diego, CA), antiphosphotyrosine (Upstate Biotechnology, Lake Placid, NY), and anti-STAT5 (Transduction Laboratories, Lexington, KY) mouse monoclonal antibodies. Then, the blots were stained by horseradish peroxidase–conjugated anti–rabbit or anti–mouse immunoglobulin G (IgG) and IgM secondary antibodies (MBL, Nagoya, Japan), respectively, and subjected to enhanced chemiluminescence detection (Amersham Life Science, Arlington Heights, IL).

Flow cytometric analysis

Cells (2×10^5) were washed with phosphate-buffered saline (PBS) and incubated with rat monoclonal antibodies specific for the mouse IL-3 receptor α chain (5B11)[38] or the mouse IL-3 receptor β chain (AIC2A; β_{IL3}; 9D3)[39] on ice for 30 minutes. Cells were washed with PBS and stained with a fluorescein isothiocyanate (FITC)–conjugated goat anti–rat IgG (Jackson Immuno Research Laboratories, West Grove, PA). For detection of the common β chain of the IL-3 receptor (AIC2B; β_C), cells were incubated with an anti–mouse β_C chain hamster monoclonal antibody (MBL), followed by incubation with an FITC-conjugated goat anti–hamster IgG secondary antibody (Jackson Immuno Research Laboratories). Cells were analyzed by flow cytometry (FACS Calibar; Becton Dickinson, San Jose, CA).

Northern blot analysis

Total cellular RNA was isolated by the guanidinium-cesium chloride method. RNA samples (approximately 20 μg per lane) were separated by

electrophoresis in 1% agarose gel containing 2.2 M formaldehyde, transferred to nylon membranes, and hybridized with the appropriate probes according to the standard procedure. For Northern blot analysis of multiple human hematolymphoid tissues, the blot was purchased from Clontech (Palo Alto, CA). Unique cDNA probes in the 3′ untranslated region of the PAR genes,[40] a 1.3-kilobase (kb) *Xho*I fragment of mouse IL-3 receptor α-chain cDNA, and a 0.8-kb *Xho*I/*Bam*HI fragment of mouse IL-3 receptor β_{IL3} chain cDNA were used as probes.

Analysis of gene expression in subsets of hematopoietic stem and progenitor cells

Cells (5×10^3) with surface marker expression patterns typical of hematopoietic stem cells (HSCs) and various types of myeloid and lymphoid progenitors were sorted from mouse bone marrow by fluorescence-activated cell sorting (FACS), as previously described.[41] Total RNA was prepared with TRIZOL reagent and subjected to cDNA synthesis with the SuperScript first-strand cDNA synthesis system (GIBCO, Carlsbad, CA). PCR was performed for 40 cycles of 94°C for 30 seconds, 55°C for 45 seconds, and 72°C for 45seconds with the following primers: 5′-ACCATCTTCCTCTACTGCCATCTTTCAG and 5′-GTACTTGGTCTCGTACTTGGACACGATG for first-round PCR; 5′-GTGATCTGGTTCTCCTTCAG for nested PCR amplification of *Tef;* and 5′-CACAGGACTAGAACACCTGC and 5′-GCTGGTGAAAAGGACCTCT for PCR amplification of *Hprt*.

Electrophoretic mobility shift assay

Binding reactions in electrophoretic mobility shift assay (EMSA) were performed with a ^{32}P–end-labeled DNA oligonucleotide probe (2×10^4 counts per minute [cpm]) in 10 μL of binding buffer (12% glycerol, 12 mM HEPES [*N*-2-hydroxyethylpiperazine-*N*′-2-ethanesulfonic acid, pH 7.9], 4 mM Tris [pH 7.9], 133 mM KCl, 300 mg of bovine serum albumin per milliliter) and 5 μL of nuclear proteins extracted from FL5.12 cells by standard procedures, as previously described.[35,42] The oligonucleotide probes used were wild-type HLF consensus sequence (CS) (5′-GCTACATATTACGTAATAAGCGTT-3′); wild-type β-casein for STAT5 (5′-AGATTTCTAGGAATTCAATCC-3′); and mutant β-casein (5′-AGATTTAGTTTAATTCAATCC-3′). As a carrier DNA, 1.5 μg of sheared calf thymus DNA or poly-d(I)d(C) was added to the reaction mixture testing for binding to HLF-CS or β-casein probe, respectively. The entire mixture was incubated at 30°C for 15 minutes. In the competition inhibition experiments, an approximately 100-fold molar excess of the unlabeled oligonucleotide was added to the reaction mixture. One microliter of polyvalent HLF(C) antiserum or preimmune rabbit serum was added to the nuclear lysates and incubated at 4°C for 30 minutes prior to the DNA-binding reaction. Nondenaturing polyacrylamide gels containing 4% acrylamide and 2.5% glycerol were prerun at 4°C in a high–ionic-strength Tris-glycine buffer for 30 minutes, loaded with the samples containing protein–DNA complexes, run at 35 mA for approximately 90 minutes, dried under vacuum, and analyzed by autoradiography.

Results

Expression of *TEF* in hematolymphoid tissues

The 3 members of the PAR family of proteins are differentially expressed in tissues and organs.[8,10,40] In contrast to HLF, which shows tissue-specific expression, TEF and DBP are expressed ubiquitously, although their expression in normal hematopoietic and lymphoid tissues has not been clarified. First, we performed Northern blot analysis of human hematolymphoid tissues using a specific cDNA probe. As shown in Figure 2A, *TEF* was expressed in the spleen, lymph node, thymus, and fetal liver but was nearly undetectable in peripheral blood leukocytes and bone marrow. *DBP* was widely expressed in hematolymphoid tissues, whereas *HLF* was expressed in the fetal liver alone. Second, subsets of mouse hematolymphoid progenitors were sorted from the bone marrow and were subjected to reverse transcriptase–PCR (RT-PCR) for *Tef* (Figure 2B).[22] Although *Tef* was detectable in unpurified bone marrow mononuclear cells, the RT-PCR product was virtually undetectable in each subset of progenitors (Figure 2B top panel). Upon performing nested PCR using each PCR product as a template, *Tef* was detected in each subset (Figure 2B middle panel). These results suggested that *Tef* is expressed in hematolymphoid progenitors but its expression is low or restricted to a small fraction of each subset of progenitors.

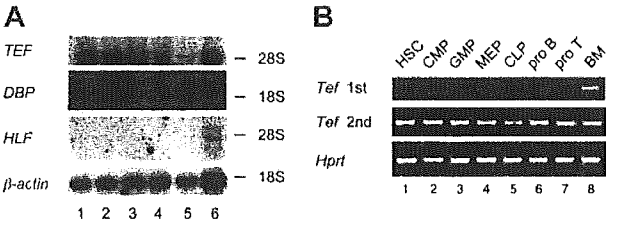

Figure 2. Expression of *TEF* during hematopoiesis. (A) Northern blot analysis of human hematolymphoid tissues. The blot was hybridized with human *TEF, DBP, HLF,* and β-actin cDNA probes. Lane 1, spleen; lane 2, lymph node; lane 3, thymus; lane 4, peripheral blood leukocyte; lane 5, bone marrow (BM); and lane 6, fetal liver. The mobility of 28S and 18S rRNA was indicated. (B) Patterns of *Tef* expression in murine myeloid and lymphoid progenitors in different stages of development. cDNA was synthesized from total RNA extracted from 5000 cells of each hematopoietic progenitor subset that had been sorted from bone marrows by FACS (lanes 1-7) as well as unpurified bone marrow mononuclear cells (lane 8). The cDNA was subjected to PCR with primers specific for the murine *Tef* (top panel) and *Hprt* (bottom panel) genes. The PCR product of amplification of *Tef* was subjected to nested PCR (middle panel). HSC indicates hematopoietic stem cells; CMP, common myeloid progenitor; GMP, granulocyte-monocyte progenitor; MEP, megakaryocyte-erythrocyte progenitor; and CLP, common lymphoid progenitor.

Establishment of FL5.12 cells conditionally expressing TEF

To analyze the function of TEF in hematopoietic cells, we established FL5.12 cells that inducibly expressed TEF by the addition of Zn using an expression vector (pMT-CB6$^+$) under the control of a metallothionein promoter. Immunoblot analysis using the anti-HLF(C) antibody that effectively recognizes HLF, DBP, and TEF proteins[34] revealed the induction of TEF protein in cells transfected with pMT-TEF when cultured in medium containing 100 μM Zn (Figure 3A lane 4). No endogenous or leaky expression of TEF protein was detected (Figure 3A lanes 1-3). Time course analysis revealed that protein expression of TEF was detectable within 4 hours after the addition of Zn (Figure 3B lane 2) and that it reached a plateau after 16 hours (Figure 3B lanes 4-5). The expression level of TEF was related to the concentration of Zn. Upon the addition of 75 μM Zn, the TEF expression level was approximately 20% of that induced by 100 μM Zn (Figure 3C lanes 4-5), whereas no significant induction was obtained by the addition of less than 50 μM Zn (Figure 3C lanes 2-3). We also established FL5.12 cells that conditionally expressed TEF/BX (Figure 3A lanes 5-6), which is a mutant form of TEF (see "Constructions of eukaryotic expression vectors"), or E2A-HLF (Figure 3A lanes 7 and 8). EMSA using the HLF-CS probe that contains the consensus binding sequence of the PAR proteins[17] detected specific protein-DNA complexes in nuclear extracts from cells expressing either TEF (Figure 3D lanes 3-4) or E2A-HLF (Figure 3D lanes 7-8) but not in nuclear extracts from cells expressing TEF/BX (Figure 3D lanes 5-6). The lack of DNA-binding ability of TEF/BX was not due to aberrant subcellular localization because immunofluorescence studies showed that TEF/BX was localized in the nucleus (data not shown).

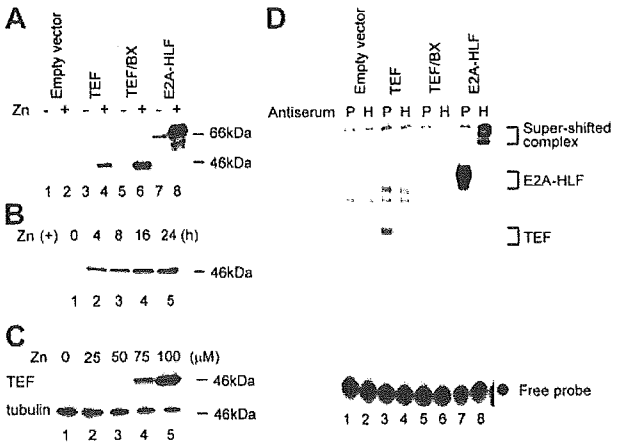

Figure 3. Establishment of FL5.12 cells conditionally expressing TEF, TEF/BX, or E2A-HLF. (A) Immunoblot analysis of FL5.12 cells using HLF(C) antiserum. Representative pools of FL5.12 cells transfected with the empty vector (lanes 1-2), pMT-TEF (lanes 3-4), pMT-TEF/BX (lanes 5-6), or pMT–E2A-HLF (lanes 7-8) were cultured in the presence (even lanes) or absence (odd lanes) of 100 μM $ZnSO_4$ for 16 hours. (B) Time course analysis of TEF expression in pMT-TEF–transfected FL5.12 cells. FL5.12 cells transfected with pMT-TEF were cultured in IL-3–containing medium in the presence of 100 μM Zn for the indicated periods of time and subjected to immunoblot analysis using the HLF(C) antiserum. (C) TEF protein expression in pMT-TEF–transfected FL5.12 cells cultured in the presence of different concentrations of Zn. FL5.12 cells transfected with pMT-TEF were cultured in the presence of Zn at the indicated concentrations for 16 hours and subjected to immunoblot analysis using the HLF(C) antiserum. The expression of tubulin was also analyzed as control. (D) Antibody-perturbed electrophoretic mobility shift analysis (EMSA) with the HLF-CS probe. FL5.12 cells transfected with the empty vector (lanes 1-2), pMT-TEF (lanes 3-4), pMT-TEF/BX (lanes 5-6), or pMT–E2A-HLF (lanes 7-8) were cultured with 100μM of Zn for 16 hours. Nuclear extracts from these cells were incubated with either preimmune (P; odd lanes) or anti-HLF(C) (H; even lanes) antiserum. Brackets show the mobility of DNA-protein complexes containing the indicated proteins and the ● indicates unbound, labeled oligonucleotide probes.

TEF but not E2A-HLF induced G_0/G_1 arrest

When TEF expression was induced by the addition of Zn in proliferating pMT-TEF–transfected FL5.12 cells cultured in IL-3–containing medium, cell growth was gradually disturbed and finally arrested within 36 hours (Figure 4A). In the dye exclusion assay, the viability of TEF-transfected cells was over 90% at 60 hours after the addition of Zn (data not shown). Growth arrest was observed when the Zn concentration was higher than 75 μM (Figure 4B). Cells transfected with pMT-TEF/BX or the empty vector proliferated exponentially in culture medium containing 100 μM Zn (Figure 4A), indicating that the growth inhibition depends on the sequence-specific DNA-binding activity of TEF and not on the cytotoxic effects of Zn. Cells transfected with pMT–E2A-HLF grew more slowly than cells transfected with the empty vector but did not undergo growth arrest (Figure 4A). Growth arrest observed in pMT-TEF–transfected FL5.12 cells was reversible after the withdrawal of Zn (Figure 4C). Cells preincubated in IL-3–containing medium in the presence of 100 μM Zn for 12 hours were washed with medium and subsequently cultured in IL-3–containing medium either in the presence or absence of 100 μM Zn. The expression of TEF was gradually decreased and became undetectable 72 hours after withdrawal of Zn (Figure 4D lanes 3, 5, 7), whereas TEF levels were maintained in the cells that were continued in culture in the presence of Zn (Figure 4D lanes 2, 4, 6). Interestingly, the growth arrest of cells cultured in the absence of Zn was reversed and cells began cycling approximately 72 hours after withdrawal of Zn, whereas the growth arrest and cell viability were maintained in the cells cultured in the presence of Zn (Figure 4C). Moreover, the growth of cells rescued by the withdrawal of Zn could be arrested again upon the subsequent readdition of Zn (Figure 4C).

To determine the cause of growth arrest, cell cycle analysis was performed using flow cytometry (Table 1). Upon the addition of Zn, TEF-expressing cells in the G_0/G_1 phase gradually accumulated and nearly 80% of the cells were in the resting phase after 48 hours. On the other hand, it was unlikely that cell death contributed to this growth arrest because the population in the sub-G_0/G_1 phase always comprised less than 10% of TEF-expressing cells (data not shown). In addition, the G_0/G_1-arrested pMT-TEF–transfected FL5.12 cells were capable of re-entering the cell cycle when Zn was withdrawn from the culture medium (Figure 4E). By contrast, in cells transfected with the empty vector, regardless of the presence or absence of Zn, more than 50% of the cells were in the S phase whereas nearly 40% of the cells were in the G_0/G_1 phase. Consistent with the slow growth rate, the number of E2A-HLF–expressing cells in the S phase slightly decreased after the addition of Zn.

TEF and E2A-HLF promoted cell survival

Next, we analyzed cell viability in the absence of IL-3 (Figure 4F). Cells were precultured in the presence or absence of Zn in IL-3–containing medium for 16 hours, washed with IL-3–free medium twice, and cultured in IL-3–free medium with or without Zn. Cells expressing E2A-HLF survived more than 72 hours in IL-3–free medium, as previously reported.[18,19] TEF also promoted cell survival in IL-3–free medium for 48 hours, but the number of viable cells gradually decreased after 72 hours even though TEF expression was maintained (data not shown). Cells expressing TEF/BX rapidly underwent apoptosis in a manner similar to that of the control cells transfected with the empty vector. These data indicated that TEF protects IL-3–dependent FL5.12 cells from apoptosis in the absence of the cytokine and that this activity depends on its DNA-binding activity.

TEF inactivated IL-3 signaling pathways

To clarify the mechanism of G_0/G_1 arrest induced by TEF, we analyzed the tyrosine phosphorylation of cellular proteins. TEF-transfected cells were preincubated in IL-3–containing medium with Zn for 18 hours, then incubated in IL-3–deficient medium with Zn for 12 hours, and then restimulated by IL-3. As previously reported by others,[43-45] rapid tyrosine phosphorylation of a wide variety of proteins was observed in cells transfected with the empty vector (Figure 5A lanes 1-4) but not in cells expressing TEF (Figure 5A lanes 5-8), suggesting that TEF inactivated signals from the IL-3 receptor. To verify the observation made in Figure 5A more precisely, we analyzed the STAT5 pathway, MAPK pathway, and phosphatidylinositol 3-kinase (PI3K) pathway by monitoring the phosphorylation status of not only STAT5[46] and p44/42 MAPK[47] but also p70S6K[48] and Akt,[49] which are downstream proteins in the PI3K pathway[47] (Figure 5B). Each FL5.12 transfectant was cultured in IL-3–free medium in the presence or absence of Zn for 12 hours following 18 hours' preincubation in IL-3–containing medium with or without Zn, respectively; subsequently exposed to IL-3 for 5 minutes; and processed for immunoblot analysis. In the absence of Zn, IL-3 stimulation of cells transfected with pMT-TEF (Figure 5B lanes 3-4) as well as cells transfected with pMT-TEF/BX (Figure 5B lanes 5-6), pMT–E2A-HLF (Figure 5B lanes 7-8), or the empty vector (Figure 5B lanes 1-2) rapidly induced the phosphorylation of STAT5. In the presence of Zn, phosphorylation of STAT5 was completely abrogated in cells

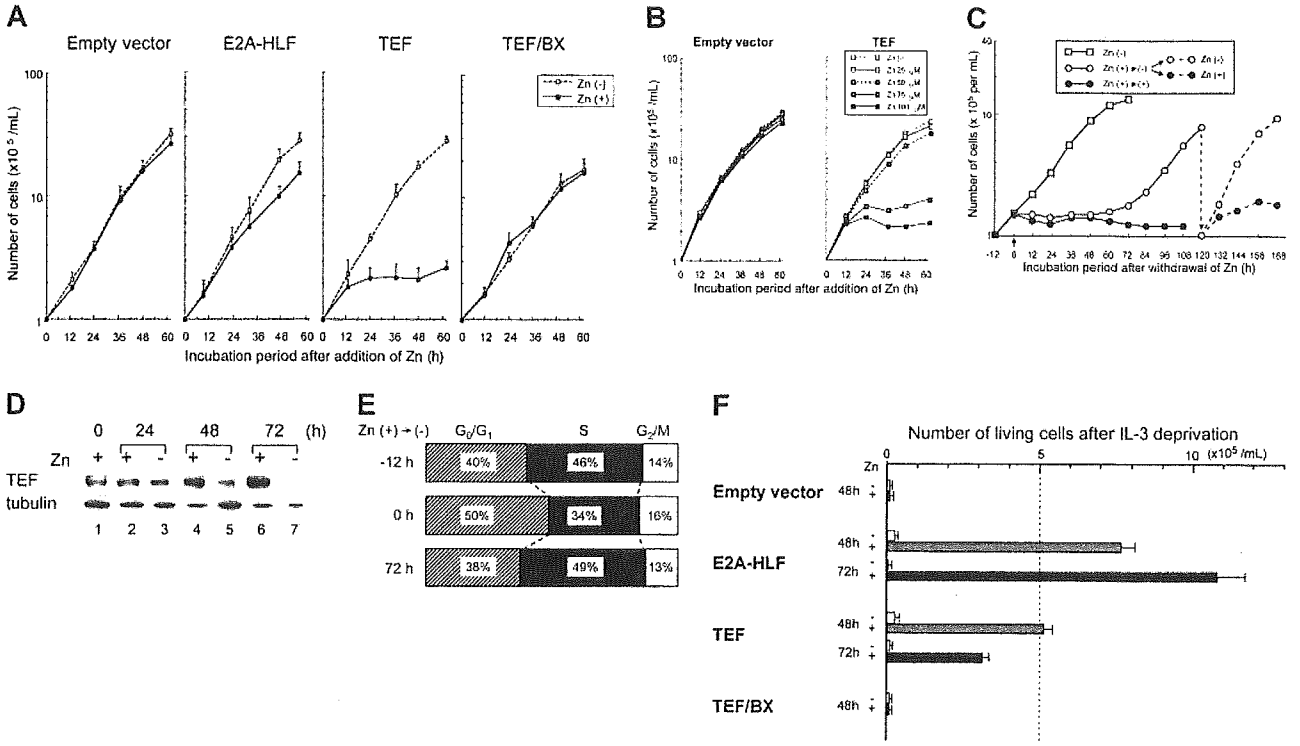

Figure 4. Growth arrest and cell survival of FL5.12 cells transfected with the TEF expression vector. (A) Growth curves of FL5.12 cells transfected with the empty vector, pMT-TEF, pMT-TEF/BX, or pMT–E2A-HLF. Cells were adjusted to 1 × 10^5 cells per mL and cultured in IL-3–containing medium in the presence (●) or absence (○) of 100 μM Zn. Representative data of multiple experiments using 3 independent pools are shown. Bars indicate standard error. (B) Growth of FL5.12 cells transfected with the empty vector or pMT-TEF in IL-3–containing medium in the presence of 0, 25, 50, 75, or 100 μM of Zn. (C) Growth curves of pMT-TEF–transfected FL5.12 cells after withdrawal of Zn. □ indicates the growth of cells cultured in IL-3–containing medium in the absence of Zn. Cells were preincubated in the presence of 100 μM Zn for 12 hours, washed with medium, adjusted to 1.5 × 10^5 cells per mL, and then cultured in IL-3–containing medium either in the presence (●) or absence (○) of 100 μM Zn. One hundred twenty hours after withdrawal of Zn, cells cultured in the absence of Zn were adjusted to 1 × 10^5 cells per mL and cultured in the presence (●- - -●) or absence (○- - -○) of 100 μM Zn. The means of triplicate samples are indicated. (D) Time course analysis of TEF expression in pMT-TEF–transfected FL5.12 cells after withdrawal of Zn. Cells were preincubated in the presence of 100 μM Zn for 12 hours, washed with medium (lane 1), then cultured in IL-3–containing medium in the presence (lanes 2, 4, and 6) or absence (lanes 3, 5, and 7) of 100 μM Zn for the indicated periods of time and subjected to immunoblot analysis using the HLF(C) antiserum. The expression of tubulin was also analyzed as control. (E) Cell cycle analysis of pMT-TEF–transfected FL5.12 cells. Cells cultured in IL-3–containing medium (top; − 12 hours) were preincubated with 100 μM of Zn for 12 hours (middle; 0 hour), washed with medium, and subsequently cultured in IL-3–containing medium in the absence of Zn for 72 hours (bottom; 72 hours). ▨ indicates G_0/G_1; ■, S; and □, G_2/M. (F) Number of viable cells after IL-3 deprivation of FL5.12 cells. FL5.12 cells transfected with the empty vector, pMT-TEF, pMT-TEF/BX, or pMT–E2A-HLF were precultured in IL-3–containing medium in the presence or absence of 100 μM of Zn for 16 hours. Cells were then washed with IL-3–free medium, adjusted to 5 × 10^5 cells per mL, and cultured without IL-3 either in the presence (▨ and ■) or absence (□) of Zn, respectively. Upon deprivation of IL-3 for 48 or 72 hours, the numbers of viable cells as determined by trypan-blue dye exclusion are indicated. The mean data of 3 independent experiments are shown. Bars indicate standard error.

transfected with the TEF expression vector (Figure 5B lanes 11-12), whereas it was rapidly induced in the other transfectants (Figure 5B lanes 9-10 and 13-16). The same results were observed with regard to the phosphorylation of p44/42 MAPK, p70S6K, and Akt. These results indicated that TEF, acting through its DNA-binding activity, blocked IL-3–signaling pathways whereas E2A-HLF did not. This was supported by the results of EMSA (Figure 5C), which demonstrated rapid induction of protein–DNA complexes containing STAT5 following restoration of IL-3[42] in nuclear extracts from cells transfected with the empty vector (Figure 5C lanes 1-6) but not in cells transfected with pMT-TEF (Figure 5C lanes 7-10).

TEF induces down-regulation of the IL-3 receptor β chains

The inactivation of IL-3 signaling observed in Figure 5 could be explained by down-regulation of the IL-3 receptor by TEF. In mice, the high-affinity IL-3 receptor is a heterodimer of the IL-3–specific α chain and either of the β_{IL3} chain or the β_C chain, the latter of which is shared with the IL-5 and granulocyte-macrophage

Table 1. Cell-cycle analysis of FL5.12 cells in the presence of IL-3

	Empty vector, %			TEF, %			E2A-HLF, %		
Zn⁺, h*	G_0/G_1	S	G_2/M	G_0/G_1	S	G_2/M	G_0/G_1	S	G_2/M
0	37	56	7	32	54	14	30	63	7
8	ND	ND	ND	39	43	17	ND	ND	ND
16	ND	ND	ND	54	27	18	ND	ND	ND
24	41	52	7	61	19	20	47	40	13
48	39	53	8	79	9	12	35	50	14

Data of representative pools of each transfectant are indicated.
ND indicates not determined.
*Hours of incubation with Zn.

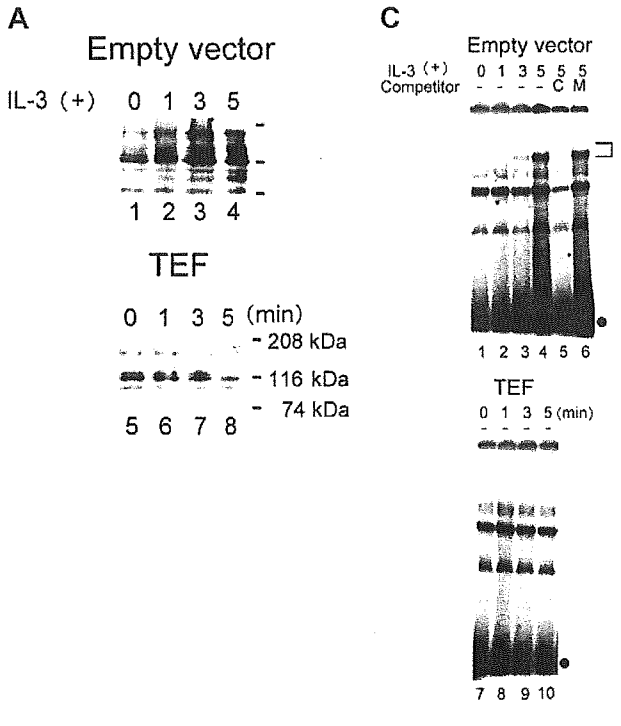

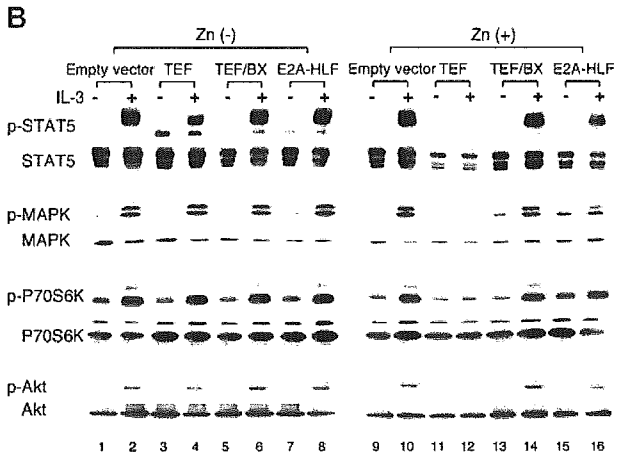

Figure 5. Phosphorylation of cellular proteins by IL-3 restoration. FL5.12 cells transfected with the empty vector, pMT-TEF, pMT-TEF/BX, or pMT–E2A-HLF were cultured in IL-3–containing medium in the presence or absence of Zn for 16 hours, and then the cells were transferred to IL-3–deficient medium in the presence or absence of Zn for 12 hours. Thereafter, cells were restimulated with IL-3 for the indicated periods of time. (A) Immunoblot analysis of FL5.12 cells that had been transfected with the empty vector (lanes 1-4) or pMT-TEF (lanes 5-8) and then cultured in IL-3–containing medium in the presence of Zn using an antiphosphotyrosine monoclonal antibody. (B) Immunoblot analysis for the phosphorylated (p) and nonphosphorylated forms of STAT5, p44/42 MAPK, p70S6K, and Akt in transfectants that had been restored with IL-3 for 5 minutes in the absence (lanes 1-8) or the presence (lanes 9-16) of Zn. The blots were probed with antiphospho-STAT5, antiphospho-p44/42 MAPK, antiphospho-p70 S6K, and antiphospho-Akt as well as anti-STAT5, anti-p44/42 MAPK, anti-p70S6K, and anti-Akt antibodies. (C) Activation of STAT5 DNA-binding by IL-3 restoration. EMSA was performed using nuclear lysates from FL5.12 cells that had been transfected with either the empty vector (lanes 1-6) or pMT-TEF (lanes 7-10) with a β-casein sequence as a probe. In the competition inhibition, an approximately 100-fold molar excess of the unlabeled β-casein sequence oligonucleotide (C; lane 5) or β-casein sequence oligonucleotide with mismatches (M; lane 6) was added in the reaction mixture. A bracket indicates the mobility of specific DNA-protein complexes and ● indicates unbound, labeled oligonucleotide probes.

colony-stimulating factor (GM-CSF) receptors.[50] Northern blot analysis was performed using an α-chain cDNA probe and a β_{IL3} chain cDNA probe; the latter recognizes both the β_{IL3} and β_C transcripts because of their extremely high levels of sequence identity (Figure 6A).[51] Upon the addition of Zn to TEF-transfected cells, the mRNA level of the β chains rapidly decreased and was almost undetectable within 16 hours. In contrast, the addition of Zn to cells transfected with either the empty vector or pMT-TEF did not change the expression level of α-chain mRNA.

Next, we analyzed the cell surface expression of the β_{IL3}, β_C, and α chains of the IL-3 receptor by flow cytometry using specific antibodies for each chain (Figure 6B). Consistent with the results of Northern blot analysis, within 24 hours after the addition of Zn, nearly complete down-regulation of the expression of both the β_{IL3} and β_C chains was observed in cells transfected with pMT-TEF but not in cells transfected with the empty vector, pMT–E2A-HLF, or pMT-TEF/BX. These data indicated that TEF down-regulates expression of the β chains in a DNA-binding–dependent fashion. Moreover, we found up-regulation of the expression of the α chain in TEF-expressing cells but not in cells transfected with the empty vector, pMT-TEF/BX, or pMT-E2A-HLF. Since Northern blot

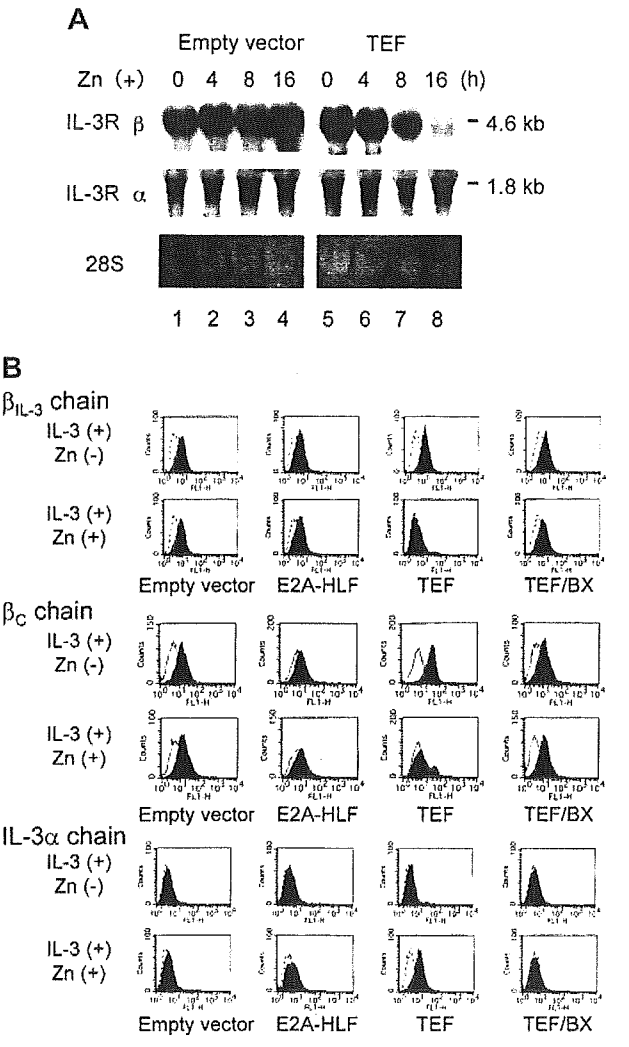

Figure 6. Northern blot analysis and flow cytometric analysis of FL5.12 cells. (A) Northern blot analysis for the IL-3 receptor. Total RNA was extracted from FL5.12 cells that had been transfected with the empty vector (lanes 1-4) or pMT-TEF (lanes 5-8) and cultured in the presence of IL-3 with Zn for the indicated periods of time. The blot was hybridized with mouse cDNA probes specific for IL-3 receptor β chains and α chain. The 28S rRNA visualized with ethidium bromide staining is shown in the bottom panel. (B) Flow cytometric analysis for surface expression of the IL-3 receptor. FL5.12 cells transfected with the empty vector, pMT–E2A-HLF, pMT-TEF, or pMT-TEF/BX were cultured in IL-3–containing medium in the presence or absence of Zn for 24 hours. Cells were analyzed with the specific antibodies for mouse β_{IL3}, β_C, or α chains. Dotted or solid lines indicate the histograms of control staining, and filled curves indicate those of specific antibodies.

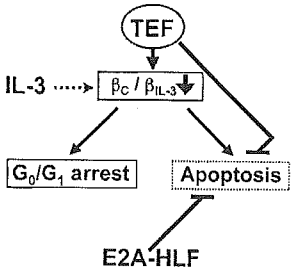

Figure 7. Hypothetical roles of TEF and E2A-HLF. TEF down-regulates the expression of the common β (β_C) chain and inactivates IL-3 signaling pathways, which are critical for both cell proliferation and cell survival. In addition, TEF promotes cell survival in the absence of survival signalings downstream of IL-3. Consequently, cells in the G_0/G_1 phase accumulated without undergoing apoptosis. In contrast, E2A-HLF blocks apoptosis without regulating the expression of cytokine receptors.

analysis revealed that the level of mRNA expression of the α chain did not change (Figure 6A), up-regulation of the cell surface α-chain expression by TEF was due to posttranscriptional mechanism(s), probably inhibition of internalization caused by down-regulation of the expression of β chains.[52] These observations indicated that TEF disrupts formation of the IL-3 receptor by down-regulating the cell surface expression of the β chains, thus rendering FL5.12 cells insensitive to IL-3.

Discussion

In this study, using a Zn-inducible system, TEF protein expression was induced in pMT-TEF–transfected FL5.12 cells within 4 hours after the addition of Zn (Figure 3B). The mRNA expression levels of the β subunits of the IL-3 receptor were reduced and became barely detectable within 16 hours (Figure 6A), and surface expression of the β chains was almost completely down-regulated within 24 hours (Figure 6B). Subsequently, the IL-3 signaling pathways were lost (Figure 5) and cells underwent cell cycle arrest in G_0/G_1 phase within 36 hours (Figure 4A; Table 1). However, the cells did not undergo apoptosis (Figure 4A) because TEF protected FL5.12 cells from apoptosis induced by IL-3 deprivation (Figure 4F). Thus, TEF induced FL5.12 cells to remain in a resting state, either in the presence or absence of IL-3 (Figure 7). These unique functions of TEF depended on its DNA-binding potential because a TEF mutant with amino acid substitutions in its basic region (TEF-BX) completely lost these activities (Figures 4-6). However, there is no potential binding site for TEF in the promoter regions of the 2 β-chain genes in the mouse[51,53] and TEF is known as a transcriptional activator.[29,37] Thus, TEF likely down-regulates transcription of the β-chain genes indirectly.

The β_C chain is common to the receptors of a series of major cytokines including IL-5 and GM-CSF as well as IL-3 and is expressed by the majority of hematopoietic progenitors (H.I. and A.K., unpublished observation, May 2004; Militi et al[54]), which expand in response to multiple growth factors during normal hematopoiesis. Therefore, it is reasonable that the *Tef* expression level in each hematolymphoid progenitor was low (Figure 2B). TEF expression may be restricted to a small fraction of progenitors that are in the resting phase and do not express the β_C chain. TEF might play an important role in preventing the exhaustion of hematopoietic progenitors by rendering a portion of the progenitors to be insensitive to growth factors. Establishment of Tef-deficient mice and extensive analysis of their hematopoiesis would elucidate the biologic significance of this unique transcription factor that regulates both cell survival and expression of cytokine receptors in hematopoietic progenitors.

This study also provides insights into functional differences between oncogenic chimeras and their normal counterparts. Similar to TEF, the E2A-HLF chimera inhibited apoptosis caused by IL-3 deprivation (Figure 4F; Inaba et al,[18] Inukai et al,[19] Altura et al[20]). However, unlike TEF, E2A-HLF did not down-regulate the expression of β subunits of the IL-3 receptor. As a result, cells expressing E2A-HLF proliferated in the presence of IL-3 (Figure 4A) and survived in the absence of IL-3 (Figure 4F). These findings suggest that the chimeric transcription factor retains the ability to drive leukemic transformation with maximum efficiency by disrupting multiple transcriptional networks. Since TEF and HLF share a high degree of sequence identity in their bZIP domains, the difference in the ability to regulate the levels of growth factor receptors between TEF and E2A-HLF is most likely caused by differences in their *trans*-activation domains (Figure 1). Alternatively, subtle changes in their DNA-binding specificity might contribute to the loss of activity of E2A-HLF to regulate cytokine receptors. The DNA-binding specificity of the PAR bZIP transcription factors is reported to be influenced by the sequences flanking the basic region, such as the basic region extension (BRE), fork region, and PAR domains.[36] Because the BRE and PAR domains of HLF are not included in the E2A-HLF chimera (Figure 1), the DNA-binding potential of E2A-HLF to suboptimal sites is substantially impaired.[34]

The antiapoptotic potential of TEF that depends on its DNA-binding activity supports a model that the consensus binding sequence recognized by the PAR factors as well as E2A-HLF, E4BP4, and CES-2 could serve as a regulatory switch for programmed cell death.[18-20,23,24] However, the detailed downstream pathways in mammalian systems have not yet been elucidated. In *C elegans*, CES-2 appears to down-regulate CES-1 expression.[5,6] Although we previously identified the *SLUG* gene, a mammalian homologue of CES-1, as one of the downstream responders of E2A-HLF in human leukemia cells with t(17;19) translocation,[23] neither TEF nor E2A-HLF was able to induce its expression in FL5.12 cells (data not shown). Thus, there must be other critical downstream pathway(s) for the antiapoptotic potential of TEF and E2A-HLF. Identification of downstream pathway(s) of TEF for its antiapoptotic potential and β_{IL3} and β_C chain gene regulation will be critical for clarifying transcriptional regulation driving normal hematopoiesis as well as leukemogenesis by E2A-HLF.

Acknowledgments

We are indebted to Dr F. Rauscher III for providing the pMT-CB6+ Zn inducible vector. This research was supported by grants-in-aid from the Ministry of Education, Science and Culture of Japan.

References

1. Horvitz HR, Shahan S, Hengarter MO. The genetics of programmed cell death in the nematode *Caenorhabditis elegans*. Cold Spring Harb Symp Quant Biol. 1994;59:377-385.
2. Ellis RE, Horvitz HR. Two *C. elegans* genes control the programmed deaths of specific cells in the pharynx. Development. 1991;112:591-603.
3. Metzstein M, Hengartner M, Tsung N, Ellis R, Horvitz HR. Transcriptional regulator of programmed cell death encoded by *Caenorhabditis elegans* gene *ces-2*. Nature. 1996;382:545-547.
4. Metzstein M, Horvitz HR. The *C. elegans* cell death specification gene ces-1 encodes a Snail family Zn finger protein. Mol Cell. 1999;4:309-319.

5. Conradt B, Horvitz HR. The *C. elegans* protein EGL-1 is required for programmed cell death and interacts with the Bcl-2-like protein CED-9. Cell. 1998;93:519-529.
6. Jacobson MD. Programmed cell death: a missing link is found. Trends In Cell Biol. 1997;7:467-469.
7. Thellmann M, Hatzold J, Conradt B. The Snail-like CES-1 protein of *C. elegans* can block the expression of the *BH3-only* cell-death activator gene *egl-1* by antagonizing the function of bHLH proteins. Development. 2003;130:4057-4071.
8. Hunger S, Ohyashiki K, Toyama K, Cleary M. Hlf, a novel hepatic bZIP protein, shows altered DNA-binding properties following fusion to E2A in t(17; 19) acute lymphoblastic leukemia. Genes Dev. 1992;6:1608-1620.
9. Hunger S. Chromosomal translocation involving the *E2A* gene in acute lymphoblastic leukemia: clinical features and molecular pathogenesis. Blood. 1996;87:1211-1224.
10. Inaba T, Roberts M, Shapiro L, et al. Fusion of the leucine zipper gene *HLF* to the *E2A* gene in human acute B-lineage leukemia. Science. 1992; 257:531-534.
11. Yoshihara T, Inaba T, Shapiro L, Kato J, Look AT. E2A-HLF-mediated cell transformation requires both the transactivation domains of E2A and the leucine zipper dimerization domain of HLF. Mol Cell Biol. 1995;15:3247-3255.
12. Inukai T, Inaba T, Yoshihara T, Look AT. Cell transformation mediated by homodimeric E2A-HLF transcription factors. Mol Cell Biol. 1997;17:1417-1424.
13. Matsunaga T, Inaba T, Matsui H, et al. Regulation of annexin II by cytokine-initiated signaling pathways and E2A-HLF oncoprotein. Blood. 2004; 103:3185-3191.
14. Kurosawa H, Goi K, Inukai T, et al. Two candidate downstream target genes for E2A-HLF. Blood. 1999;93:321-332.
15. Dang J, Inukai T, Kurosawa H, et al. The-E2A-HLF oncoprotein activates groucho-related genes and suppresses runx1. Mol Cell Biol. 2001;21: 5935-5945.
16. Honda H, Inaba T, Suzuki T, et al. Expression of E2A-HLF chimeric protein induced T-cell apoptosis, B-cell maturation arrest, and development of acute lymphoblastic leukemia. Blood. 1999;93: 2780-2790.
17. Smith KS, Rhee JW, Naumovski L, Cleary ML. Disrupted differentiation and oncogenic transformation of lymphoid progenitors in E2A-HLF transgenic mice. Mol Cell Biol. 1999;19:4443-4451.
18. Inaba T, Inukai T, Yoshihara T, et al. Reversal of apoptosis by the leukaemia-associated E2A-HLF chimeric transcriptional factor. Nature. 1996;382: 541-544.
19. Inukai T, Inaba T, Ikushima S, Look AT. Antiapoptotic role of the AD1 and AD2 transactivation domains of E2A in pro-B lymphocytes deprived of growth factor. Mol Cell Biol. 1998;18:6035-6043.
20. Altura R, Inukai T, Ashmun R, et al. The chimeric E2A-HLF transcription factor abrogates p53-induced apoptosis in myeloid leukemia cells. Blood. 1998;92:1397-1405.
21. Inukai T, Inoue A, Kurosawa H, et al. *SLUG*, a *ces-1*-related Zn-finger transcription factor gene with antiapoptotic activity, is a downstream target of the E2A-HLF oncoprotein. Mol Cell. 1999;4: 343-352.
22. Inoue A, Seidel MG, Wu W, et al. Slug, a highly conserved zinc finger transcriptional repressor, protects hematopoietic progenitor cells from radiation-induced apoptosis in vivo. Cancer Cell. 2002;2:279-288.
23. Ikushima S, Inukai T, Inaba T, et al. Pivotal role of the NFIL3/E4BP4 transcription factor in interleukin 3-mediated survival of pro-B lymphocytes. Proc Natl Acad Sci U S A. 1997;94:2609-2614.
24. Kuribara R, Kinoshita T, Miyajima A, et al. Two distinct interleukin-3-mediated signal pathways, Ras-NFIL3 (E4BP4) and Bcl-x_L, regulate the survival of murine pro-B lymphocytes. Mol Cell Biol. 1999;19:2754-2767.
25. Drolet D, Scully K, Simmons D, et al. TEF, a transcription factor expressed specifically in the anterior pituitary during embryogenesis, defines a new class of leucine zipper proteins. Genes Dev. 1991;5:1739-1753.
26. Mueller CR, Maire P, Schibler U. DBP, a liver-enriched transcriptional activator, is expressed late in ontogeny and its tissue specificity is determined posttranscriptionally. Cell. 1990;61:279-291.
27. Wuarin J, Schibler U. Expression of the liver-enriched transcriptional activator protein DBP follows a stringent circadian rhythm. Cell. 1990;63: 1257-1266.
28. Falvey E, Fleury-Olela F, Schibler U. The rat hepatic leukemia factor (HLF) gene encodes two transcriptional activators with distinct circadian rhythms, tissue distributions and target preferences. EMBO J. 1995;14:4307-4313.
29. Fonjallaz P, Ossipow V, Wanner G, Schibler U. The two PAR leucine zipper proteins, TEF and DBP, display similar circadian and tissue-specific expression, but have different target promoter preferences. EMBO J. 1996;15:351-362.
30. Lopez-Molina L, Conquet F, Dubois-Dauphin M, Schibler U. The DBP gene is expressed according to a circadian rhythm in the suprachiasmatic nucleus and influences circadian behavior. EMBO J. 1997;16:6762-6771.
31. Balsalobre A, Damiola F, Schibler U. A serum shock induces circadian gene expression in mammalian tissue culture cells. Cell. 1998;93: 929-937.
32. Yamaguchi S, Mitsui S, Yan L, et al. Role of DBP in the circadian oscillatory mechanism. Mol Cell Biol. 2000;20:4773-4781.
33. Mitsui S, Yamaguchi S, Matsuo T, Ishida Y, Okamura H. Antagonistic role of E4BP4 and PAR proteins in the circadian oscillatory mechanism. Genes Dev. 2001;15:995-1006.
34. Hunger S, Brown R, Cleary M. DNA-binding and transcriptional regulatory properties of hepatic leukemia factor (HLF) and the t(17;19) acute lymphoblastic leukemia chimera E2A-HLF. Mol Cell Biol. 1994;14:5986-5996.
35. Inaba T, Shapiro L, Funabiki T, et al. DNA-binding specificity and trans-activating potential of the leukemia-associated E2A-hepatic leukemia factor fusion protein. Mol Cell Biol. 1994;14:3403-3413.
36. Haas N, Cantwell C, Johnson P, Burch J. DNA-binding specificity of the PAR basic leucine zipper protein VBP partially overlaps those of the C/EBP and CREB/ATF families and is influenced by domains that flank the core basic region. Mol Cell Biol. 1995;15:1923-1932.
37. Hunger S, Li S, Fall M, Naumovski L, Cleary M. The proto-oncogene HLF and the related basic leucine zipper protein TEF display highly similar DNA-binding and transcriptional regulatory properties. Blood. 1996;87:4607-4617.
38. Hara T, Miyajima A. Two distinct functional high affinity receptors for mouse interleukin-3 (IL-3). EMBO J. 1992;11:1875-1884.
39. Ogorochi T, Hara T, Wang H, Maruyama K, Miyajima A. Monoclonal antibodies specific for low-affinity interleukin-3 (IL-3) binding protein AIC2A: evidence that AIC2A is a component of a high-affinity IL-3 receptor. Blood. 1992;79:895-903.
40. Khatib Z, Inaba T, Valentine M, Look AT. Chromosomal localization and cDNA cloning of the human DBP and TEF genes. Genomics. 1994;23: 344-351.
41. Akashi K, Traver D, Miyamoto T, Weissman IL. A clonogenic common myeloid progenitor that give rise to all myeloid lineages. Nature. 2000;404: 193-197.
42. Mui A, Wakao H, O'Farrell A, Harada N, Miyajima A. Interleukin-3, granulocyte-macrophage colony stimulating factor and interleukin-5 transduce signals through two STAT5 homologs. EMBO J. 1995; 14:1166-1175.
43. Isfort R, Huhn R, Frackelton A, Ihle J. Stimulation of factor-dependent myeloid cell lines with interleukin 3 induces tyrosine phosphorylation of several cellular substrates. J Biol Chem. 1988;35: 19203-19209.
44. Duronio V, Clark-Lewis I, Federsppiel B, Wieler J, Schrader J. Tyrosine phosphorylation of receptor beta subunits and common substrates in response to interleukin-3 and granulocyte-macrophage colony-stimulating factor. J Biol Chem. 1992;30:21856-21863.
45. Silvennoinen O, Witthuhn B, Quelle F, Cleveland J, Ihle J. Structure of the murine Jak2 protein-tyrosine kinase and its role in interleukin 3 signal transduction. Proc Natl Acad Sci U S A. 1993;90: 8429-8433.
46. Dumon S, Santos SC, Debierre-Grockiego F, et al. IL-3 dependent regulation of Bcl-xL gene expression by STAT5 in a bone marrow derived cell line. Oncogene. 1999;18:4191-4199.
47. Kinoshita T, Miyajima A. Raf/MAPK and rapamycin-sensitive pathway mediate the anti-apoptotic function of p21Ras in IL-3-dependent hematopoietic cells. Oncogene. 1997;15:619-627.
48. Reif K, Burgering B, Cantrell D. Phosphatidylinositol 3-kinase links the interleukin-2 receptor to protein kinase B and p70 S6 kinase. J Biol Chem. 1997;272:14426-14433.
49. Dudek H, Datta SR, Franke TF, et al. Regulation of neuronal survival by the serine-threonine protein kinase Akt. Science. 1997;275:661-665.
50. Miyajima A, Mui AL, Ogorochi T, Sakamaki K. Receptor for granulocyte-macrophage colony-stimulating factor, interleukin-3, and interleukin-5. Blood. 1993;82:1960-1974.
51. Gorman D, Itoh N, Jenkins N, et al. Chromosomal localization and organization of the murine genes encoding the β subunits (AIC2A and AIC2B) of the interleukin 3, granulocyte/macrophage colony-stimulating factor, and interleukin 5 receptors. J Biol Chem. 1992;22:15842-15848.
52. Algate P, Steelman L, Mayo M, Miyajima A, McCubrey J. Regulation of the interleukin-3 (IL-3) receptor by IL-3 in the fetal liver-derived FL5.12 cell line. Blood. 1994;83:2459-2468.
53. van Dijk T, Baltus B, Caldenhoven E, et al. Cloning and characterization of the human interleukin-3 (IL-3)/IL-5/granulocyte-macrophage colony-stimulating factor receptor βc gene: regulation by Ets family members. Blood. 1998;92:3636-3646.
54. Militi S, Riccioni R, Parolini I, et al. Expression of interleukin 3 and granulocyte-macrophage colony-stimulating factor receptor common chain β_C, β_{IT} in normal hematopoiesis: lineage specificity and proliferation-independent induction. Br J Hematol. 2000;111:441-451.

ARTHRITIS & RHEUMATISM
Vol. 52, No. 1, January 2005, pp 164–170
DOI 10.1002/art.20739

Repair of Articular Cartilage Defect by Autologous Transplantation of Basic Fibroblast Growth Factor Gene–Transduced Chondrocytes With Adeno-Associated Virus Vector

Naoki Yokoo,[1] Tomoyuki Saito,[1] Masaaki Uesugi,[1] Naomi Kobayashi,[1] Ke-Qin Xin,[1] Kenji Okuda,[1] Hiroaki Mizukami,[2] Keiya Ozawa,[2] and Tomihisa Koshino[1]

Objective. **To examine the effects of basic fibroblast growth factor (bFGF) gene–transduced chondrocytes on the repair of articular cartilage defects.**

Methods. **LacZ gene or bFGF gene was transduced into primary isolated rabbit chondrocytes with the use of a recombinant adeno-associated virus (AAV) vector. These gene-transduced chondrocytes were embedded in collagen gel and transplanted into a full-thickness defect in the articular cartilage of the patellar groove of a rabbit. The efficiency of gene transduction was assessed according to the percentage of LacZ-positive cells among the total number of living cells. The concentration of bFGF in the culture supernatant was measured by enzyme-linked immunosorbent assay to confirm the production by bFGF gene–transduced chondrocytes. At 4, 8, and 12 weeks after transplantation, cartilage repair was evaluated histologically and graded semiquantitatively using a histologic scoring system ranging from 0 (complete regeneration) to 14 (no regeneration) points.**

Results. **LacZ gene expression by chondrocytes was maintained until 8 weeks in >85% of the in vitro population. LacZ-positive cells were found at the transplant sites for at least 4 weeks after surgery. The mean concentration of bFGF was significantly increased in bFGF gene–transduced cells compared with control cells ($P < 0.01$). Semiquantitative histologic scoring indicated that the total score was significantly lower in the bFGF-transduced group than in the control group throughout the observation period.**

Conclusion. **These results demonstrated that gene transfer to chondrocytes by an ex vivo method was established with the AAV vector, and transplantation of bFGF gene–transduced chondrocytes had a clear beneficial effect on the repair of rabbit articular cartilage defects.**

Damage of articular cartilage leads to joint dysfunction associated with pain or limited range of motion and usually progresses to degeneration of the articular surface, resulting in osteoarthritis. It is well recognized that articular cartilage is a highly differentiated tissue with a limited capacity for self-repair. Current therapy for osteoarthritis consists of short-acting antiinflammatory drugs, intraarticular injection of steroids or other agents, such as hyaluronic acid, and surgical intervention. However, these treatments may not relieve joint pain completely. Therefore, cartilage repair seems to be essential for the prevention of a catastrophic outcome in a joint. Several studies describing the successful repair of osteochondral defects by the transplantation of cultured chondrocytes have been reported (1). However, a major problem with cartilage repair by autologous chondrocyte transplantation is that a large quantity of chondrocytes from normal articular cartilage is required, whereas donor sites have a limited capacity to provide chondrocytes.

Supported by a grant-in-aid for Scientific Research and by the Yokohama Foundation for the Advancement of Medical Science.

[1]Naoki Yokoo, MD, Tomoyuki Saito, MD, PhD, Masaaki Uesugi, MD, PhD, Naomi Kobayashi, MD, Ke-Qin Xin, MD, PhD, Kenji Okuda, MD, PhD, Tomihisa Koshino, MD, PhD: Yokohama City University School of Medicine, Yokohama, Japan; [2]Hiroaki Mizukami, MD, PhD, Keiya Ozawa, MD, PhD: Jichi Medical School, Tochigi, Japan.

Address correspondence and reprint requests to Naoki Yokoo, MD, Department of Orthopaedic Surgery, Yokohama City University School of Medicine, 3-9 Fukuura, Kanazawa-ku, Yokohama 236-0004, Japan. E-mail: Napoleon@nyc.odn.ne.jp.

Submitted for publication February 4, 2004; accepted in revised form September 27, 2004.

Many studies have demonstrated that basic fibroblast growth factor (bFGF) is one of the most potent of the various growth factors for cartilage repair (2–6). In order to establish an efficient approach for the treatment of cartilage defects, it may be advantageous to maintain a certain level of growth factor locally for a long time.

A new therapeutic approach to cartilage repair, gene therapy, has been described, in which genes are transduced into chondrocytes with the use of naked DNA or viral vectors (7–10). However, problems with this method are related to the ability to obtain high-efficiency transduction, to maintain long-term expression of the therapeutic gene, and safety. Recently, the adeno-associated virus (AAV) has been recognized as a tool for transducing a gene into target cells (11–14). Gene therapy with AAV has several advantages, including the lack of virulence of the wild-type virus, the safety, since there is no replication activity alone, the ability to transduce to nondividing cells, the integration into the host genome, and the long-term expression of the transduced gene.

In this study, we attempted to use this new delivery vector to repair cartilage defects, in an ex vivo method. The purpose of this study was to evaluate the utility of the AAV vector for ex vivo gene delivery to chondrocytes and to investigate the repair of an articular cartilage defect by transplantation of bFGF gene–transduced chondrocytes.

MATERIALS AND METHODS

AAV vector production. Two AAV constructs were prepared for this study: AAV-LacZ contained the bacterial β-galactosidase (LacZ) gene and AAV-bFGF contained the bFGF gene, which harbors a nuclear localization signal under the regulation of the cytomegalovirus immediate early promoter. The AAV subtype 2 vector plasmid used in this study, pLacZ, was derived from the vector plasmid pW1, which contains the LacZ gene, as previously described (15). Recombinant bFGF gene (GenBank accession no. X07285) was obtained from Takeda Chemical Industries (Osaka, Japan). A fragment containing bFGF complementary DNA was amplified by polymerase chain reaction using the following primer pairs with the *Eco* RI or the *Xho* I site: 5′-ATGAATTCATGGCTGCCGGCAGCATCACTTCGCTT-3′ and 5′-ATCTCGAGAGAGTCAGCTCTTAGCAGAC-3′. The fragment was subcloned between the *Eco* RI and *Xho* I sites of the pLacZ AAV vector plasmid to replace the LacZ gene (pbFGF). An AAV helper plasmid containing subtype 2 AAV *rep* and *cap* genes, which are required for replication and capsid formation of AAV vectors, pIM45 was used. A plasmid containing the E2A, E4, and VA genes of the adenovirus genome, pladeno-1, was used in place of helper adenovirus for AAV vector production.

Subconfluent human fetal kidney cells (293 cells) were cotransfected by the calcium phosphate coprecipitation method with pbFGF, pIM45, and pladeno-1 to produce the AAV-inducing bFGF gene (AAV-bFGF). After 48 hours, the cells were harvested and lysed in Tris HCl buffer (10 m*M* Tris HCl, 150 m*M* NaCl, pH 8.0) through 3 cycles of freezing and thawing. One round of sucrose precipitation and 2 rounds of CsCl density-gradient ultracentrifugation were performed to isolate AAV-bFGF from the lysates. The vector titer was determined by quantitative DNA dot-blot hybridization of the DNase I–resistant fraction.

Isolation of chondrocytes. Thirty-nine 10-week-old Japanese white rabbits (Oriental Yeast Company, Tokyo, Japan), weighing an average of 1.8 kg, were used in this study. They were divided into 3 groups: 9 for the LacZ-transduced group, 12 for the bFGF-transduced group, and 18 for the control group. Under intravenous anesthesia with pentobarbital sodium (Somnopentyl; Schering-Plough, Union, NJ), articular cartilage tissues (4 × 4–mm slices) were harvested from the patellar groove of the right knee, washed 3 times in phosphate buffered saline (PBS), and cut into small pieces. The pieces were treated with 0.05% trypsin and 0.001*M* EDTA (Gibco BRL, Gaithersburg, MD) for 30 minutes at 37°C and digested sequentially with 0.25% collagenase (type II collagenase; Worthington, Lakewood, NJ) for 3 hours at 37°C. The isolated chondrocytes were washed 3 times with PBS.

The mean number of cells collected from each rabbit was 2.4×10^5 (SD 0.5×10^5). These cells were divided into 4–6 culture wells and cultured in 24-well flat-bottomed plates (Falcon, Lincoln Park, NJ) at a concentration of 5×10^4 cells/well in 0.5 ml of Dulbecco's modified Eagle's medium (DMEM; Sigma, St. Louis, MO) supplemented with 10% fetal calf serum (FCS) and antibiotics (100 units/ml of penicillin G, 0.1 mg/ml of streptomycin; Gibco BRL) (DMEM–FCS), at 37°C in an atmosphere of 5% CO_2 in air.

Gene transduction into chondrocytes. Chondrocytes were cultured for 3 days, removed from the growth medium, and washed once with serum-free medium. To the culture wells for the transduced group was added 500 μl of serum-free DMEM containing AAV-LacZ or AAV-bFGF to enable quantification of transgene expression at the optimal number of viral particles (10^5 particles per cell) determined from the LacZ gene group experiments. To culture wells for the control group was added 500 μl of serum-free DMEM containing Tris buffer alone. After incubation for 1 hour at 37°C, 500 μl of DMEM–FCS was added to each culture well for both culture groups. One sample from each rabbit was used for autologous transplantation. The remaining samples were used for in vitro experiments.

Twenty samples from the LacZ-transduced group and 20 from the control group were used for the experiment to determine the efficacy of gene transduction in vitro. Culture medium was exchanged twice a week after gene transduction up to the time of analysis. At 3, 7, 14, 28, and 56 days after transduction, LacZ expression was assessed using the X-Gal staining technique (16), as follows. Cells were washed 3 times with PBS and fixed with 0.5% glutaraldehyde for 10 minutes, followed by 2 rinses in PBS containing 1 mmole/liter of $MgCl_2$. The cells were finally incubated with X-Gal substrate (1 mg/ml of X-Gal, 1 mmole/liter of $MgCl_2$, 5 mmoles/liter of $K_4Fe[CN]_6/K_3Fe[CN]_6$ in PBS) for 12 hours at 37°C. Efficiency of gene transduction was calculated as the average percentage

of X-Gal–positive cells per total number of living cells in 3 randomly selected fields viewed with an optical microscope.

Measurement of bFGF concentration in culture medium. Samples from 12 rabbits in the bFGF-transduced group and from 12 rabbits in the control group were used for determinations of accumulated bFGF production in the culture supernatant. The culture medium was not changed at each sampling of either group. At 3, 7, and 14 days after transduction, culture supernatants were collected from every 4 bFGF-transduced or control group culture wells, respectively, and after centrifugation, were stored at –80°C until analyzed. The bFGF concentration in the culture supernatants was measured by enzyme-linked immunosorbent assay (ELISA) using a bFGF-specific ELISA kit (Quantikine; R&D Systems, Minneapolis, MN) according to the manufacturer's instructions.

Autologous transplantation of gene-transduced chondrocytes into an articular cartilage defect. Chondrocytes from the LacZ-transduced, bFGF-transduced, and control groups were cultured for 1 week after gene transduction, collected from the culture wells by trypsinization, and then centrifuged. The supernatant was removed, and chondrocytes were embedded in a 0.2% solution of type I collagen (Cellgen; Koken, Tokyo, Japan) at a density of 1×10^6/ml. For autologous transplantation, chondrocytes were suspended in the collagen gel by incubation at 37°C for 1 hour.

Rabbits were anesthetized with pentobarbital sodium, and the left hind leg of each rabbit was sterilized for surgery. A 3-cm medial parapatellar incision was made over the knee, and the patella was dislocated laterally. A full-thickness defect in the articular cartilage (5 mm in diameter; 3 mm deep) was made in the patellar groove using a hand drill. The collagen gel containing $\sim 7.5 \times 10^4$ autologous chondrocytes was transplanted into the full-thickness defect. A periosteal flap of $\sim 5 \times 5$ mm was harvested from the anteromedial surface of the tibia and sutured to the peripheral rim of the artificial defect with 5-0 nylon thread. The cambium layer of the periosteal flap was faced toward the joint space. The rabbits were allowed to move freely immediately after surgery.

Among the 39 rabbits, LacZ-transduced chondrocytes were transplanted into 9, bFGF-transduced chondrocytes into 12, and chondrocytes without gene transduction into the remaining 18.

Evaluation of LacZ expression at the site of transplantation. Rabbits from the LacZ-transduced (n = 3) and control (n = 2) groups were killed at 1, 2, and 4 weeks after transplantation. The specimens were harvested from the patellar groove, embedded in TissueTek OCT compound (Sakura Finetek USA, Torrance, CA), and immediately frozen in nitrogen liquid. The frozen specimens were sectioned into 20-μm slices with a cryotome (Coldtome CM-502; Sakura Seiki, Tokyo, Japan) and double-stained with X-Gal and hematoxylin and eosin (H&E).

Histologic evaluation of repair cartilage. Rabbits from the bFGF-transduced (n = 4) and control (n = 4) groups were killed at 4, 8, and 12 weeks after transplantation. The distal part of the femur was resected en bloc, fixed with 10% buffered formalin, and decalcified with a 0.5*M* EDTA solution. Sagittal sections were prepared and stained with H&E, toluidine blue, or Safranin O–fast green. The histologic features of each specimen were evaluated semiquantitatively using the histologic scoring system described by Wakitani et al (17). This system consists of 5 categories (cell morphology, matrix staining, surface regularity, cartilage thickness, and integration of donor with host) scored on a 0–14-point scale, where 0 = complete regeneration and 14 = no regeneration.

Statistical analysis. Data are expressed as the mean ± SD. The statistical significance of differences was calculated with the use of StatView software (version J-5.0; Abacus Concepts, Berkeley, CA). One-way analysis of variance and the Mann-Whitney U test were used for analyzing statistical significance. *P* values less than 0.05 were considered significant.

RESULTS

In vitro experiment. *Efficiency of gene transduction of chondrocytes.* The efficiency of gene transduction was determined for chondrocytes transfected with AAV-LacZ at 7 days after transduction. The mean ± SD percentage of LacZ-positive cells among the total number of living cells was 43.7 ± 8.8%, 62.4 ± 5.1%, 97.7 ± 0.6%, and 98.2 ± 1.5% at a vector dose of 10^3, 10^4, 10^5, and 10^6 particles/cell, respectively (Figure 1). The percentage of successfully transduced chondrocytes increased in a vector dose–dependent manner. A vector dose of $>10^6$ particles/cell did not improve the transduction rate. The optimal dose of virus that was required to achieve transduction of ~100% of the chondrocytes was determined to be 10^5 particles/cell.

LacZ gene expression was highly maintained until 56 days after gene transduction. The mean ± SD percentage of LacZ-positive cells was 69.4 ± 15.1%, 97.7 ± 0.6%, 97.2 ± 1.8%, 95.8 ± 2.9%, and 85.8 ± 6.2% at 3, 7, 14, 28, and 56 days after transduction, respectively (Figure 2). The greatest population of

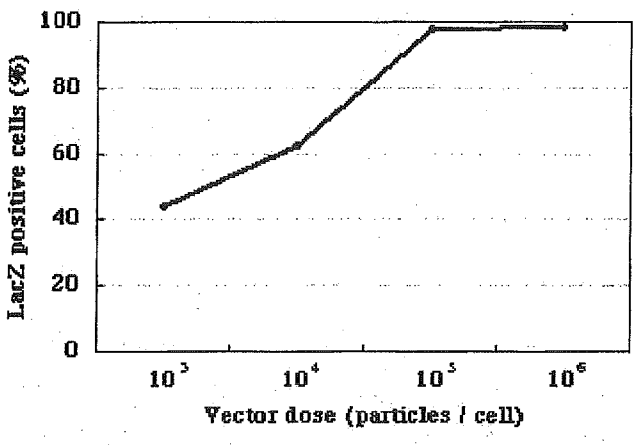

Figure 1. Vector dose–dependent LacZ expression in cultured chondrocytes. On day 7 after adeno-associated virus–LacZ transduction into chondrocytes, LacZ expression was assessed by X-Gal staining. The percentages of LacZ-positive cells among the total number of living cells were 43.7%, 62.4%, 97.7%, and 98.2% at doses of 10^3, 10^4, 10^5, and 10^6 particles/cell, respectively.

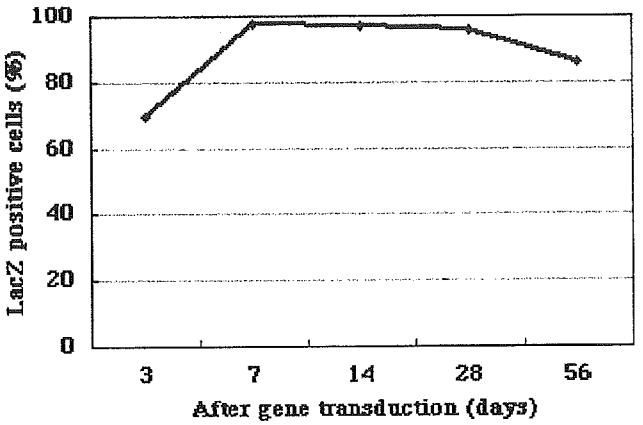

Figure 2. Time-dependent expression of LacZ in cultured chondrocytes. The percentages of LacZ-positive cells were 69.4%, 97.7%, 97.2%, 95.8%, and 85.8% at 3, 7, 14, 28, and 56 days after transduction, respectively.

LacZ-expressing cells was 97.7% at 7 days (Figure 3A), and more than 85% of the population was maintained up to 56 days. Cells without LacZ transduction in the control group failed to reveal LacZ expression at any sampling point (Figure 3B). There was no microscopic evidence of cell death or cytopathologic changes in the transduced cells as determined by optical microscopy.

Expression of bFGF gene by transduced chondrocytes. Production of bFGF was detected in both bFGF-transduced cells and control cells. The mean ± SD bFGF concentration in culture supernatants from the bFGF-transduced cells was 88.2 ± 9.8 ng/ml, 130.9 ± 28.8 ng/ml, and 240.6 ± 22.5 ng/ml at 3, 7, and 14 days after transduction, respectively (Figure 4). In control

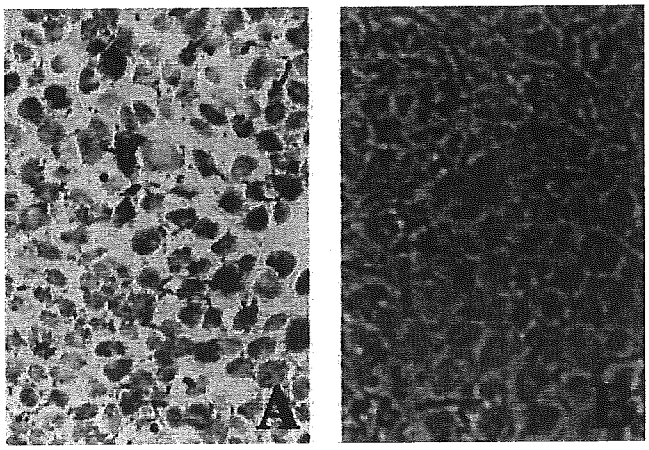

Figure 3. Photomicrographs of transduced chondrocytes stained with X-Gal. **A,** LacZ group chondrocytes were stained with X-Gal on day 7 after adeno-associated virus–LacZ transduction. LacZ-positive cells are stained blue. **B,** Control group chondrocytes showed no LacZ-positive cells. (Original magnification × 100.)

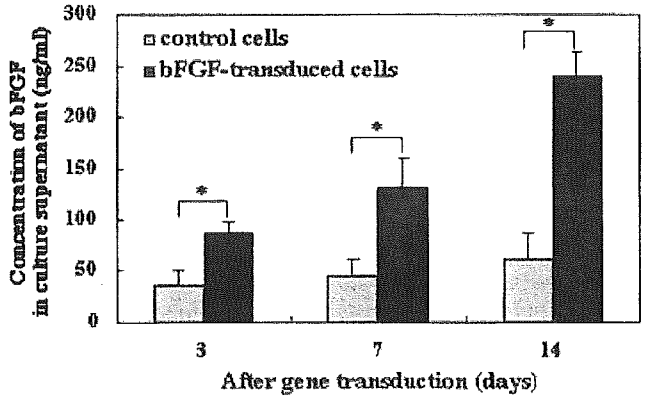

Figure 4. Concentration of basic fibroblast growth factor (bFGF) in culture supernatants of bFGF-transduced chondrocytes. Culture supernatants of control and bFGF-transduced cells were collected on days 3, 7, and 14 after transduction, and the bFGF concentration was determined by enzyme-linked immunosorbent assay. Transduction of the bFGF gene significantly elevated the secretion of bFGF (* = $P <$ 0.01).

cells, the bFGF concentration was 35.0 ± 15.8 ng/ml, 44.5 ± 16.4 ng/ml, and 62.3 ± 25.8 ng/ml at 3, 7, and 14 days after transduction, respectively. The bFGF concentration was significantly greater in bFGF-transduced cells than in the control cells on all sampling days ($P <$ 0.01).

The mean number of chondrocytes in the bFGF-transduced group was 14.1×10^4 (SD 1.1×10^4) and 34.8×10^4 (SD 6.2×10^4) at 7 and 14 days after transduction, respectively. In the control group, the numbers were 6.4×10^4 (SD 1.5×10^4) and 17.0×10^4 (SD 3.2×10^4) at 7 and 14 days after transduction, respectively. The mean number of chondrocytes in the bFGF-transduced group was significantly higher than that in the control group during the period of culture ($P < 0.01$).

In vivo experiment. *LacZ expression at the transplant site.* Throughout the observation period, X-Gal staining of LacZ-transduced cells showed cells with blue nuclei distributed across the entire regenerated cartilage under the layer covered by the transplanted periosteal flap. The controls, which received transplants without LacZ-transduced chondrocytes, did not show LacZ-positive cells at any week of sampling. No adverse effects related to the virus were observed in this ex vivo gene transfer experiment.

Macroscopic findings at the site of transplantation of the bFGF-transduced chondrocytes. Macroscopic observation of the transplant site showed regeneration of the articular cartilage defect in both the bFGF-transduced and control groups. At 12 weeks, the margin between the regenerated tissue and the

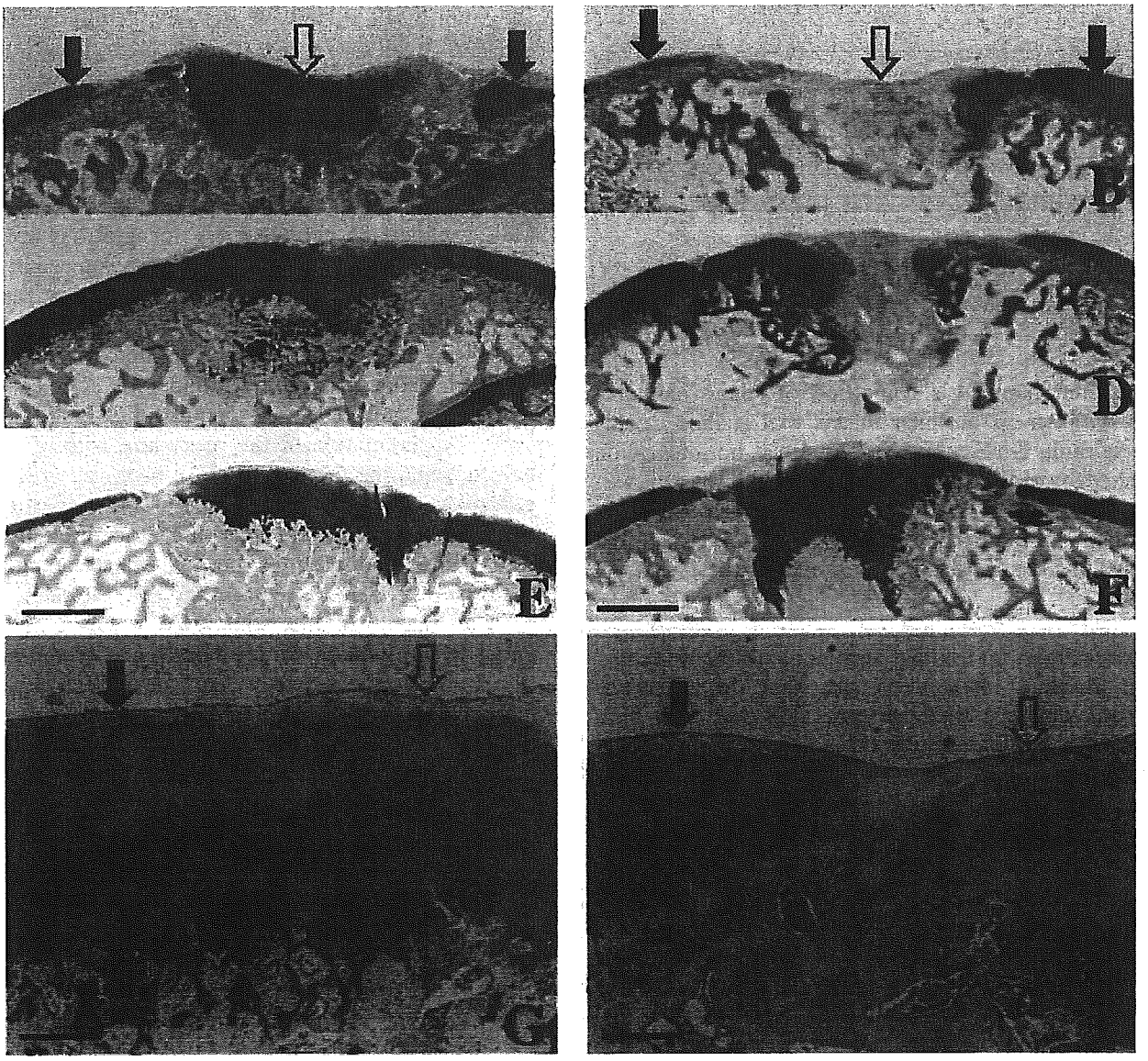

Figure 5. Photomicrographs of sagittal sections of articular cartilage defects in rabbits after transplantation with basic fibroblast growth factor (bFGF)–transduced chondrocytes (**A, C, E,** and **G**) and control chondrocytes (**B, D, F,** and **H**). Photomicrographs of the junction area are also shown (**G** and **F**). In the bFGF-transduced group, at 4 weeks (**A**), the deep layer is composed of round chondrocytes, but the matrix is weakly stained. At 8 weeks (**C**), the matrix is more distinctly stained, but the superficial region is weakly stained. At 12 weeks (**E** and **G**), the matrix is intensely metachromatically stained, and there is reconstitution of the osteochondral junction in most specimens. In the control group, at 4 weeks (**B**) and 8 weeks (**D**), the matrix is faintly stained. At 12 weeks (**F** and **H**), the deep layer of the matrix stained well, but staining is reduced in the superficial layers. **Solid arrows** indicate regenerated cartilage; **open arrows** indicate surrounding normal cartilage. Sections were stained with Safranin O–fast green. Bars in **A** and **F** = 1 mm; bars in **G** and **H** = 100 μm.

original cartilage was not distinguishable in both groups. The surface of the regenerated cartilage closely resembled normal cartilage in the bFGF-transduced group, but that in the control group could still be distinguished from surrounding normal cartilage. No sign of osteoarthrosis, such as erosion of cartilage or osteophyte formation, was seen in any of the knees during the observation period.

Histologic findings of regenerated cartilage following transplantation of bFGF-transduced chondrocytes. At 4 weeks after transplantation, in the tissues obtained from the bFGF-transduced group, the deep part of the

Table 1. Histologic scores of regenerated cartilage at 4, 8, and 12 weeks*

Weeks after transplantation	Control group	bFGF-transduced group
4	8.8 ± 1.0	6.5 ± 0.6†
8	7.0 ± 1.4	4.3 ± 1.0†
12	5.5 ± 1.7	2.8 ± 1.0†

* The histologic features were scored on a 0–14-point scale as described by Wakitani et al (17), where 0 represents complete regeneration and 14 represents no regeneration. Values are the mean ± SD. bFGF = basic fibroblast growth factor.
† $P < 0.01$ versus controls.

regenerated tissue was composed of round chondrocytes, with an extracellular matrix that stained weakly with Safranin O (Figure 5A). There was no integration of the edges of the regenerated tissue with the adjacent normal cartilage or reconstitution of the osteochondral junction in any specimen. In the control group, the extracellular matrix was faintly stained with Safranin O (Figure 5B).

At 8 weeks, the bFGF-transduced group showed an extracellular matrix that was more distinctly stained with Safranin O in the deep part, while the superficial part was weakly stained (Figure 5C). Although both edges were integrated with the adjacent normal cartilage, reconstitution of the osteochondral junction was not seen in any specimen. The tissues from the control group at 8 weeks were essentially the same as those at 4 weeks (Figure 5D).

In the bFGF-transduced group at 12 weeks, the intensity and thickness of the extracellular matrix that was metachromatically stained with Safranin O were increased as compared with the findings at 4 and 8 weeks, and the microstructure of the regenerated tissue resembled the surrounding normal cartilage (Figures 5E and G). There was reconstitution of the osteochondral junction in most of the specimens. In the control group, the deep layer of the regenerated cartilage matrix stained well with Safranin O, but staining was reduced in the superficial layers (Figures 5F and H). There was no reconstitution of the osteochondral junction in any of the control specimens.

The Wakitani score was 6.5 ± 0.6, 4.3 ± 1.0, and 2.8 ± 1.0 points (mean ± SD) at 4, 8, and 12 weeks after transplantation, respectively, in the bFGF-transduced group. In the control group, the score was 8.8 ± 1.0, 7.0 ± 1.4, and 5.5 ± 1.7 points at 4, 8, and 12 weeks after transplantation, respectively (Table 1). The scores in both groups gradually decreased throughout the experimental period. However, the score in the bFGF-transduced group became significantly lower than that in the control group with the passage of time postoperatively ($P < 0.01$).

DISCUSSION

Autologous chondrocyte transplantation has been successfully applied in recent years to the treatment of focal cartilage defects in a series of patients (18). Autologous chondrocytes for grafting are harvested from non–weight-bearing areas, cultured in vitro, reinjected into the cartilage defect, and the area is covered with a periosteal flap that is sutured in place. However, this method may be limited to small local cartilage defects, since the number of cells collected from donor sites to be used for cultivation is still limited.

Augmentation of the procedure with bFGF for help in repairing the cartilage has been reported to be efficacious (4–6,19). Weisser et al (4) reported that among several different growth factors used to treat transplanted chondrocytes, positive effects on cartilage repair were observed only with the bFGF-treated chondrocyte implants (4). Previous studies showed that exogenous bFGF induces the proliferation of chondrocytes, the maturation of cartilage, and the differentiation of mesenchymal cells, and it stimulates the synthesis of cartilaginous matrix (5,6). Otsuka et al (19) reported that continuous administration of bFGF using an osmotic pump had a clearly beneficial effect on repair of cartilage defects. However, bFGF alone did not lead to complete structural restitution of hyaline cartilage to repair the full-thickness defects of articular cartilage. Prolonged local expression of bFGF by transduction of the genetic code of bFGF into chondrocytes would be an efficient treatment for articular cartilage defects.

For the repair of cartilage defects with gene therapy, it may be necessary to obtain high-efficiency transduction and continuous local expression of the therapeutic gene. Several studies have demonstrated that the AAV vector has the ability to highly efficiently transduce a gene into cells, to integrate into the host genome, and to express the transduced gene for a long time (20–22). There are studies of the utility of the AAV vector for joint disease that demonstrated high-efficiency gene delivery to the synovium in vivo (23) or gene transduction to cultured chondrocytes in vitro (24). Delivering genes directly to the surface of the abnormal articular cartilage in order to accelerate cartilage repair could result in a long-term treatment. The advantage of ex vivo gene delivery would be direct delivery of the therapeutic gene to the abnormal articular cartilage and the ability to limit the area of gene expression to the cartilage defect alone. In our previous study, ex vivo

gene transfer to periosteum-derived cells using an AAV vector induced LacZ expression for 4 weeks in vivo (25).

In this study, high-efficiency LacZ gene transduction into chondrocytes was obtained long-term in vitro, and LacZ gene expression in vivo was sustained without any adverse effects. These findings suggest that gene transfer to an articular cartilage defect by use of the ex vivo method was established with the AAV vector. Cartilage repair was slightly inferior to that described in previous reports, even though we used 10-week-old rabbits for the experiment. One of the reasons was thought to be differentiation to fibrous chondrocytes during the 1-week culture before transplantation. The cell number and the bFGF secretion were significantly increased in bFGF-transduced chondrocytes compared with the control chondrocytes in vitro. Furthermore, the histologic appearance of the transplant site in the bFGF-transduced group was fully repaired compared with that in the control group. The repair at a comparatively early stage was apparently different between bFGF-transduced and null chondrocytes even at 12 weeks. Continuous bFGF secretion by gene transfer seemed to be an effective way to promote cartilage repair.

These results demonstrate that repair of full-thickness defects in rabbit articular cartilage can be enhanced by transplantation of bFGF gene–transduced chondrocytes. This method seems to be one of the best techniques for achieving repair of articular cartilage defects.

ACKNOWLEDGMENT

We thank Avigen, Inc. (Alameda, CA) for supplying the plasmid for the production of the AAV vector.

REFERENCES

1. Brittberg M, Lindahl A, Nilsson A, Ohlsson C, Isaksson O, Peterson L. Treatment of deep cartilage defects in the knee with autologous chondrocyte transplantation. N Engl J Med 1994;331: 889–95.
2. Kato Y, Gospodarowicz D. Sulfated proteoglycan synthesis by confluent cultures of rabbit costal chondrocytes grown in the presence of fibroblast growth factor. J Cell Biol 1985;100:477–85.
3. Hunziker EB, Rosenberg LC. Repair of partial-thickness defects in articular cartilage: cell recruitment from the synovial membrane. J Bone Joint Surg Am 1996;78:721–33.
4. Weisser J, Rahfoth B, Timmermann A, Aigner T, Brauer R, von der Mark K. Role of growth factors in rabbit articular cartilage repair by chondrocytes in agarose. Osteoarthritis Cartilage 2001; 9:48–54.
5. Shida J, Jingushi S, Izumi T, Iwaki A, Sugioka Y. Basic fibroblast growth factor stimulates articular cartilage enlargement in young rats in vivo. J Orthop Res 1996;14:265–72.
6. Cuevas P, Burgos J, Baird A. Basic fibroblast growth factor (FGF) promotes cartilage repair in vivo. Biochem Biophys Res Commun 1988;156:611–8.
7. Arai Y, Kubo T, Kobayashi K, Takeshita K, Takahashi K, Ikeda T, et al. Adenovirus vector-mediated gene transduction to chondrocytes: in vitro evaluation of therapeutic efficiency of transforming growth factor-β1 and heat shock protein 70 gene transduction. J Rheumatol 1997;24:1787–95.
8. Baragi VM, Renkiewicz RR, Qiu L, Brammer D, Riley JM, Sigler RE, et al. Transplantation of adenovirally transduced allogeneic chondrocytes into articular cartilage defects in vivo. Osteoarthritis Cartilage 1997;5:275–82.
9. Doherty PJ, Zhang H, Tremblay L, Manolopoulos V, Marshall KW. Resurfacing of articular cartilage explants with genetically-modified human chondrocytes in vitro. Osteoarthritis Cartilage 1998;6:153–9.
10. Kang BR, Marui T, Ghivizzani SC, Nita IM, Georgescu HI, Suh JK, et al. Ex vivo gene transfer to chondrocytes in full-thickness articular cartilage defects: a feasibility study. Osteoarthritis Cartilage 1997;5:139–43.
11. Schwarz EM. The adeno-associated virus vector for orthopaedic gene therapy [review]. Clin Orthop 2000;379 Suppl:S31–9.
12. Kaplitt MG, Leone P, Samulski RJ, Xiao X, Pfaff DW, O'Malley KL, et al. Long-term gene expression and phenotypic correction using adeno-associated virus vectors in the mammalian brain. Nat Genet 1994;8:148–54.
13. Xiao X, Li J, McCown TJ, Samulski RJ. Gene transfer by adeno-associated virus vectors into the central nervous system. Exp Neurol 1997;144:113–24.
14. Berns KI, Giraud C. Adenovirus and adeno-associated virus as vectors for gene therapy. Ann N Y Acad Sci 1995;772:95–104.
15. Xin KQ, Urabe M, Yang J, Nomiyama K, Mizukami H, Hamajima K, et al. A novel recombinant adeno-associated virus vaccine induces a long-term humoral immune response to HIV. Hum Gene Ther 2001;12:1047–61.
16. Price J, Turner D, Cepko C. Lineage analysis in the vertebrate nervous system by retrovirus-mediated gene transfer. Proc Natl Acad Sci U S A 1987;84:156–60.
17. Wakitani S, Goto T, Pineda SJ, Young RG, Mansour JM, Caplan AI, et al. Mesenchymal cell-based repair of large, full-thickness defects of articular cartilage. J Bone Joint Surg Am 1994;76: 579–92.
18. Richardson JB, Caterson B, Evans EH, Ashton BA, Roberts S. Repair of human articular cartilage after implantation of autologous chondrocytes. J Bone Joint Surg Br 1999;81:1064–8.
19. Otsuka Y, Mizuta H, Takagi K, Iyama K, Yoshitake Y, Nishikawa K. Requirement of fibroblast growth factor signaling for regeneration of epiphyseal morphology in rabbit full-thickness defects of articular cartilage. Dev Growth Differ 1997;39:143–56.
20. Kessler PD, Podsakoff GM, Chen X, McQuiston SA, Colosi PC, Matelis LA, et al. Gene delivery to skeletal muscle results in sustained expression and systemic delivery of a therapeutic protein. Proc Natl Acad Sci U S A 1996;93:14082–7.
21. Fisher KJ, Jooss K, Alston J, Yang Y, Haecker SE, High K, et al. Recombinant adeno-associated virus for muscle directed gene therapy. Nat Med 1997;3:306–12.
22. Herzog RW, Hastrom JN, Kung SH, Tai SJ, Wilson JM, Fisher KJ, et al. Stable gene transfer and expression of human blood coagulation factor IX after intramuscular injection of recombinant adeno-associated virus. Proc Natl Acad Sci U S A 1997;94:5804–9.
23. Goater J, Muller R, Kollias G, Firestein GS, Sanz I, O'Keefe RJ, et al. Empirical advantages of adeno associated viral vectors for in vivo gene therapy for arthritis. J Rheumatol 2000;27:983–9.
24. Arai Y, Kubo T, Fushiki S, Mazda O, Nakai H, Iwaki Y, et al. Gene delivery to human chondrocytes by an adeno associated virus vector. J Rheumatol 2000;27:979–82.
25. Kobayashi N, Koshino T, Uesugi M, Yokoo N, Xin KQ, Okuda K, et al. Gene marking in adeno-associated virus vector infected periosteum-derived cells for cartilage repair. J Rheumatol 2002; 29:2176–80.

20

Use of Simian Immunodeficiency Virus Vectors for Simian Embryonic Stem Cells

Takayuki Asano, Hiroaki Shibata, and Yutaka Hanazono

Summary

The ability to stably introduce genetic material into primate embryonic stem (ES) cells could allow broader application. In this chapter, we describe a method of gene transfer into simian (cynomolgus macaque) ES cells using a simian immunodeficiency virus-based lentivirus vector. When cynomolgus ES cells are transduced with a simian immunodeficiency virus vector encoding the green fluorescent protein (GFP) gene, a large fraction of cells (greater than 50%) fluoresce, and high levels of GFP expression persist for months as assessed by flow cytometry and real-time polymerase chain reaction. Thus, the use of GFP as a reporter gene allows direct and simple detection of successfully transduced ES cells and facilitates monitoring of ES cell proliferation and differentiation both in vitro and in vivo. In addition, this highly efficient gene transfer method allows faithful gene delivery to primate ES cells with potential for both research and therapeutic applications.

Key Words: Flow cytometry; gene transfer; green fluorescent protein; lentivirus vector; primate embryonic stem cells; real-time PCR; simian immunodeficiency virus vector.

1. Introduction

Nonhuman primate embryonic stem (ES) cells have remarkable similarities to human ES cells in all aspects, including morphology and surface marker expression. On the other hand, primate (both human and nonhuman) ES cells are quite distinct from mouse ES cells, for instance, in their growth velocity, feeder and leukemia inhibitory factor (LIF) dependency, and their morphology and surface marker expression. Therefore, experimental results using mouse ES cells may not be predictive of those in primates. These discrepancies stimulated us to use nonhuman primate (simian) ES cells as a predictive model to more closely reflect human ES cell characteristics and behavior *(1,2)*.

The lentivirus vector was first established from human immunodeficiency virus (HIV)-1 *(3)*. It can transduce quiescent cells such as neurons and hematopoietic stem cells *(3,4)*. Non-HIV lentivirus vectors have also been established by modifying feline

From: *Methods in Molecular Biology, vol. 329: Embryonic Stem Cell Protocols: Second Edition: Volume 1*
Edited by: K. Turksen © Humana Press Inc., Totowa, NJ

immunodeficiency virus, equine infectious anemia virus, simian immunodeficiency virus (SIV), or bovine immunodeficiency virus *(5–9)*. Among primate lentivirus vectors, the merit of SIV vectors over HIV-1 vectors is safety. The sequence homology between HIV-1 and SIV is considerably low (approx 50%) *(10)*. The generation of replication-competent virus by recombination between SIV vectors and HIV-1 in human subjects is therefore highly unlikely. This provides a great advantage in safety over HIV vectors, especially when target cells are already infected with HIV or permissive to HIV infection.

HIV-1-based lentivirus vectors can efficiently transduce human cells but not those of Old World monkeys *(11)*. A species-specific cytoplasmic component confers the innate postentry restriction to HIV-1 infection in simian cells *(12)*. Unlike HIV-1 vectors, SIV vectors can efficiently transduce simian embryonic and hematopoietic stem cells *(13,14)*. In this chapter, we describe a method to use a SIV-based lentivirus vector for efficient gene transfer into simian (cynomolgus macaque) ES cells.

2. Materials

2.1. Cells

1. Simian (rhesus or cynomolgus) ES cells *(1,2)*.
2. Mouse embryonic fibroblasts (MEFs) from CD-1 (also referred to as ICR [Institute of Cancer Research]) (Charles River, Wilmington, MA) or BALB/c mice (Charles River).
3. 293T human embryonic kidney cell line (ATCC, Manassas, VA; cat. no. 11268).

2.2. Culture Media and Reagents

1. Dulbecco's modified Eagle's medium (DMEM) (Sigma, St. Louis, MO; cat. no. D-6429).
2. DMEM nutrient mixture F-12 1:1 mixture (DMEM/F12) (Invitrogen, Carlsbad, CA; cat. no. 11330-032).
3. ES cell-qualified fetal bovine serum (FBS; Invitrogen, cat. no. 10439-024).
4. 10,000 IU/mL penicillin-10,000 μg/mL streptomycin (100X; Invitrogen, cat. no. 15070-063).
5. 200 m*M* L-glutamine (100X; Invitrogen, cat. no. 25030-081).
6. 2-Mercaptoethanol (Sigma, cat. no. M3148).
7. FBS (Sigma, cat. no. F-2442).
8. Phosphate-buffered saline (PBS) (Invitrogen, cat. no. 10010-023).
9. Hanks balanced salt solution (HBSS) (Invitrogen, cat. no. 14025-092).
10. 0.25% trypsin-ethylenediaminetetraacetic acid (Invitrogen, cat. no. 25200-056).
11. 2.5% trypsin (Invitrogen, cat. no. 15090-046).
12. Polybrene (Sigma, cat. no. S2667).
13. Culture medium for primate ES cells: DMEM/F12 containing 15% ES cell-qualified FBS, 2 m*M* L-glutamine, 100 IU/mL penicillin-100 μg/mL streptomycin, and 0.1 m*M* 2-mercaptoethanol.
14. Culture medium for 293T cells: DMEM containing 10% FBS and 100 IU/mL penicillin-100 μg/mL streptomycin.
15. Post-transfection medium: DMEM containing 20% FBS.

2.3. SIV Vectors

1. pVSV-G (sold as a part of the pantropic retroviral expression system; BD Biosciences Clontech, San Jose, CA; cat. no. 631512 and 631530).

2. SIV packaging plasmid and SIV gene transfer plasmid (for plasmid construction, *see* **ref. 7**).
3. Lipofectamine reagent (Invitrogen, cat. no. 18324-111).
4. Plus reagent (Invitrogen, cat. no. 11514-015).
5. Opti-MEM (Invitrogen, cat. no. 11058-021).
6. Stericup filters (Millipore, Billerica, MA; cat. no. SCHV U01RE).

2.4. Flow Cytometry

1. A flow cytometer equipped with an argon-ion laser (Becton Dickinson FACScan, FACS Caliber, or an equivalent).
2. Cell strainers (BD Falcon, San Jose, CA; cat. no. 352350).
3. Round-bottom test tubes with cell strainer caps (BD Falcon, cat. no. 352235).
4. Fluorescent-activated cell sorting (FACS) medium: 2% FBS and 0.1% NaN_3 (Wako, Osaka, Japan; cat. no. 197-11091) in PBS.
5. Fixing medium: 1% paraformaldehyde (Wako, cat. no. 064-00406) in PBS.
6. Phycoerythrin (PE)-conjugated antimouse-H-$2K^d$ monoclonal antibody (BD PharMingen, San Jose, CA; cat. no. 553566).

2.5. Real-Time Polymerase Chain Reaction

1. A real-time thermal cycler (ABI-PRISM 7000 sequence detection system or an equivalent).
2. A QIAamp DNA minikit (Qiagen, Hilden, Germany; cat. no. 51104).
3. A Quantitect SYBR green polymerase chain reaction (PCR) kit (Qiagen, cat. no. 204143).
4. MicroAmp optical 96-well reaction plates (Applied Biosystems, Foster City, CA; cat. no. N801-0560) and MicroAmp caps (Applied Biosystems, cat. no. N801-0535).
5. A spectrophotometer (Beckman Coulter DU 7500 or an equivalent).

3. Methods

3.1. Construction of SIV Vector

We have used the SIV vector derived from SIV African green monkey (SIVagm) *(7)* to transduce simian ES cells. SIV vectors can transduce simian ES cells more efficiently than adenovirus, adeno-associated virus, or oncoretrovirus vectors *(13)*. In addition, SIV vectors can efficiently transduce nondividing cells, for instance, the ocular tissue and adipocytes *(15,16)*.

Instead of depending on specific SIV entry via CD4 and other co-receptors, the vesicular stomatitis virus (VSV)-G envelope has generally been used to pseudotype SIV vectors. Because the cellular receptors for VSV-G, including phosphatidylserine, phosphatidylinositol, and GM3 ganglioside, appear to be very abundant and ubiquitous membrane components of most mammalian cells, VSV-G-enveloped viruses can infect a wide variety of cells and tissues. In addition to the broader range, VSV-G-pseudotyped viruses are physically more stable than naturally occurring lentiviruses and can be concentrated by centrifugation (*see* **Subheading 3.1.2.**).

3.1.1. Transfection

1. Dissociate exponentially growing 293T cells with 0.25% trypsin-ethylenediaminetetraacetic acid solution and plate 5×10^6 293T cells in a 100-mm plate (60–80% confluent) 1 d prior to transfection (*see* **Note 1**).
2. On the day of transfection, mix 4.5 μg of the gene transfer plasmid, 1.3 μg of the packaging plasmid, and 0.5 μg of the envelope plasmid (pVSV-G) in 750 μL of Opti-MEM.

3. Prepare the Plus reagent just prior to use and add 20 µL Plus reagent to the DNA solution (from **step 2**). Vortex gently and incubate the mixture at room temperature for 15 min.
4. Dilute 30 µL of the Lipofectamine reagent into 750 µL of OptiMEM in a separate tube.
5. Mix the DNA/Plus solution (770 µL; from **step 3**) and the Lipofectamine solution (780 µL; from **step 4**) followed by incubation at room temperature for 15 min.
6. During the incubation, replace the medium of 293T cells with 6.5 mL OptiMEM.
7. After the incubation, evenly add the DNA/Plus/Lipofectamine solution (1.55 mL total; from **step 5**) onto 293T cells and incubate the plate at 37°C, 5% CO_2. At 4 h after the transfection, add 8 mL DMEM containing 20% FBS.

3.1.2. Harvest and Concentration of Vector

1. Incubate the plate (from **Subheading 3.1.1.**) overnight and replace medium with 10 mL regular 293T growth medium.
2. At 24 h after media replacement, harvest the supernatant (which contains the vector) and filter it though a 0.45-µm pore membrane. The titer of vector will be 10^5–10^6 transducing units (TU) per milliliter (*see* **Note 2**).
3. Concentrate the vector supernatant at 42,500*g* for 2 h with a high-speed centrifuge.
4. After centrifugation, carefully discard the supernatant and resolve the pellet with PBS containing 5% FBS. The suspension volume should be 1/1000 to 1/100 of the initial volume. The final titer of vector will be 10^8–10^9 TU/mL (*see* **Note 3**).

3.2. Transduction

1. Plate 1.5×10^5 ES cells on an MEF (5×10^5 cells) feeder layer in a 35-mm dish and incubate the dish at 37°C, 5% CO_2, for 12–24 h.
2. Gently wash ES cells with HBSS and add 1 mL (half of the regular volume) of the growth medium.
3. Thaw a viral stock without foaming in a water bath at 37°C and add it to the culture (*see* **Note 4**).
4. After 10 h, aspirate the medium, gently wash ES cells once with HBSS, and replace with 2 mL fresh medium.
5. At 2–3 d after transduction, evaluate the transduction efficiency (*see* **Subheading 3.3.** and **Note 5**).

3.3. Assessment of Transduction Efficiency

After transduction, it is important to assess the transduction efficiency, usually 2–3 d after exposure to the vector. If a marker gene such as green fluorescent protein (GFP) is included in the vector, then you can assess the transduction efficiency by examining the marker gene expression. GFP expression can be easily monitored under a fluorescent microscope or by flow cytometry (*see* **Subheading 3.3.1.**). Another method to assess the transduction efficiency is to examine the SIV-provirus (vector integrated into the host genome) by real-time DNA-PCR (*see* **Subheading 3.3.2.**). It is particularly useful when marker genes are not available or marker gene expression levels are not high enough.

When cynomolgus ES cells are transduced once or twice with an SIV vector encoding the GFP gene, more than 50% of cells fluoresce, and the GFP expression persists for months. In addition, high levels of GFP expression are observed during embryoid body formation *(13)*. On the other hand, transduction of cynomolgus ES cells with an

oncoretrovirus vector results in lower gene transfer rates (less than 20%), suggesting that simian lentivirus vectors can transduce simian ES cells more efficiently than oncoretrovirus vectors *(13)*.

3.3.1. Flow Cytometry

1. Aspirate old medium from the culture and rinse cells with HBSS (from **Subheading 3.2., step 5**). Add 2 mL 0.25% trypsin-HBSS to the dish and incubate for 5 min at 37°C. Detach ES cell colonies from the bottom by tapping with your fingers. Add 3 mL ES medium to the dish, disperse the cells into single cells using a 1-mL tip, and transfer the cell suspension to a 15-mL conical tube.
2. Spin cells in a centrifuge at 140*g* for 4–5 min. Aspirate the medium and resuspend the pellet in FACS medium. Pass the cell suspension through a cell strainer to remove cell clusters (*see* **Note 6**). Count a cell number and adjust it at $1–2 \times 10^6$ cells/mL.
3. Transfer 100 µL cell suspension ($1–2 \times 10^5$ cells) into a 1.5-mL tube. Add 0.1 µg (1 µL) of PE-conjugated antimouse H-2K^d monoclonal antibody solution to the tube and incubate it for 30–60 min on ice.
4. After incubation, add 1 mL FACS medium to the tube and spin cells at 800*g* for 5 min at 4°C. Aspirate medium and wash the pellet with FACS medium. Spin the cell suspension at 800*g* for 5 min at 4°C again.
5. Resuspend the pellet with 200–500 µL fixing medium. The cell suspension can be left at 4°C overnight until flow cytometric analysis.
6. Transfer the cell suspension to a round test tube through a strainer cap.
7. Perform flow cytometric analysis using a flow cytometer with excitation at 488 nm. The fluorescence data of GFP and PE can be obtained via FL1 and FL2 parameters, respectively. **Figure 1** shows a typical profile of cynomolgus ES cells transduced with an SIV vector expressing GFP. Cynomolgus ES cells are negative for antimouse H-2K^d, but co-cultured MEF feeder cells (derived from BALB/c mice) are positive for it; thus, you can distinguish both ES and MEF cells.

3.3.2. Real-Time PCR

1. Extract DNA from a culture pellet (containing both ES and MEF cells from **Subheading 3.2., step 5**) using a QIAamp DNA minikit (*see* **Note 7**). Assess the purity of DNA by checking a 260/280-nm absorbance ratio with a spectrophotometer. Preferably, it is higher than 1.75. Adjust the concentration of DNA stocks (dilute with DNase-free water) to 50 µg/mL.
2. Prepare a master mix for real-time PCR as shown in **Table 1** (*see* **Note 8**). Dispense 45 µL into each well of a MicroAmp optical 96-well reaction plate.
3. Add 5 µL (250 ng) template DNA to each well and seal the plate with MicroAmp caps.
4. Place the plate in a real-time thermal cycler and start a PCR program.
5. Analyze data according your software package (*see* **Note 9**).

4. Notes

1. Because 293T cells were established from 293 cells after transfection with the SV40 large T antigen and neomycin resistance genes, it is recommended to treat 293T cells with 800 µg/mL (active) of G418 for 1 wk once a month so the transgenes are not lost. It is, however, important to passage 293T cells several times without G418 before virus production to avoid contamination of G418 in the viral supernatant.

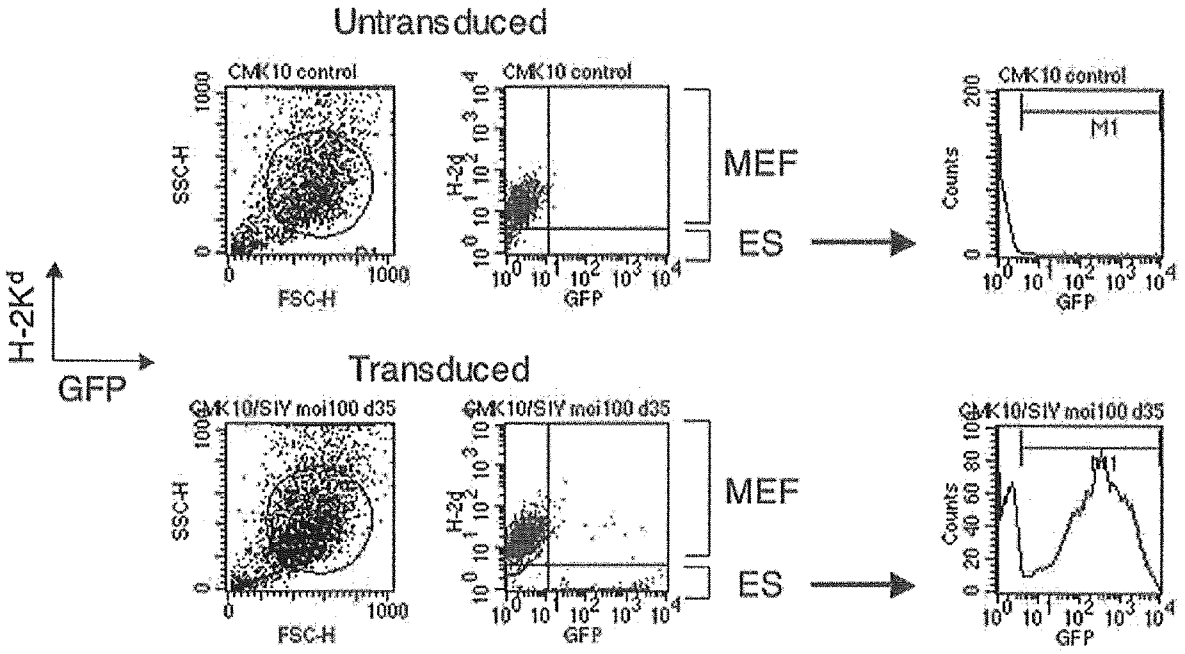

Fig. 1. Assessment of transduction efficiency by flow cytometry. The transgene green fluorescent protein (GFP) expression was analyzed on a FACScan using *CellQuest* software 2–3 d after transduction with a GFP-expressing simian immunodeficiency virus vector. The co-cultured BALB/c-derived feeder cells could be distinguished from the cynomolgus embryonic stem cells using PE-conjugated mouse antimouse H-2K^d monoclonal antibody, which does not react to cynomolgus cells but does react to BALB/c cells.

2. The titer (transducing units, TU) of vector is defined as the ability to transduce target cells. For instance, 10^5 TU/mL indicates that 1 mL vector solution is able to transduce 10^5 cells. We usually use 293T cells as targets to assess the titer. The titer of virus can also be assessed in terms of genomic copies (often designated gc). Genomic copy number of SIV vector can be evaluated by RNA dot-blot or quantitative RNA-PCR.
3. The vector solution can be stored at −80°C at least for several months. The titer will decrease even at −20°C. Frozen stocks should be thawed quickly in a water bath at 37°C just prior to use. Avoid repeated freezing and thawing, or the titer will decrease.
4. The passage of ES cells before and after lentiviral transduction is the same as the routine passage; 30–100 cells per clump is the best. You do not have to disperse clumps for transduction. Vectors are added at 10–50 TU per target cell. We sometimes add polybrene (final concentration 4–8 μg/mL) in the transduction culture and other times do not add it. It does not seem that polybrene improves the transduction efficiency with SIV vectors unlike the case with oncoretrovirus vectors. It is suggested that ES cell exposure to lentivirus solution is no longer than 12 h. Longer exposure may result in a large decrease in ES cell number, presumably because of the toxicity of the pseudotyped envelope VSV-G protein. Serum may greatly hamper lentiviral transduction. If you do not obtain good gene transfer efficiency, then it is suggested to remove the serum from your transduction culture.
5. The transgene expression in ES cells can be enhanced by changing the promoter or adding *cis*-acting elements in the vector. The *cis*-acting sequences include the central polypurine and termination tract (cPPT) to facilitate nuclear import of the viral complex and the woodchuck posttranscriptional regulatory element (WPRE) to increase transgene expression *(17)*. **Figure 2** shows variable GFP expression in cynomolgus ES cells transduced with SIV vectors containing various promoters and cPPT/WPRE sequences.